

7. SITE 580¹

Shipboard Scientific Party²

HOLE 580

Date occupied: 6 June 1982
Date departed: 8 June 1982
Time on hole: 2 days, 3 hr.
Position (latitude; longitude): 41°37.47'N; 153°58.58'E
Water depth (sea level; corrected m, echo-sounding): 5375
Water depth (rig floor; corrected m, echo-sounding): 5385
Bottom felt (m, drill pipe): 5386.7
Penetration (m): 155.3
Number of cores: 17
Total length of cored section (m): 155.3
Total core recovered (m): 140.74
Core recovery (%): 91
Oldest sediment cored:
Depth sub-bottom (m): 155.3
Nature: siliceous clay
Age: late Pliocene
Measured velocity (km/s): 1.5

Basement: Not reached

Principal results: A thick sequence of Pleistocene and late Pliocene sediments was recovered at Site 580. Siliceous microfossils (diatoms and radiolarians) are generally abundant and moderately to well preserved. An excellent magnetic reversal record can be identified back to the middle of the Gauss Normal Epoch.

One hundred and fifty-five meters of sediment were penetrated. Except for the numerous ash layers and indurated darkish green layers, these sediments are a remarkably uniform gray, olive gray, and dark gray color. Based on these data, the entire sedimentary sequence recovered at Site 580 is placed in one lithologic unit. However, based on changes in biosiliceous components and clay-sized carbonate, five subunits are recognized.

The upper subunit (Subunit IA) extends from 0 to 60.3 m sub-bottom and is predominantly a siliceous clay. Underlying this (Subunit IB) and extending from 60.3 to 79.3 m sub-bottom is a cal-

careous siliceous clay, characterized by up to 25% clay-sized carbonate material. Subunit IC (79.3–117.3 m sub-bottom) is similar lithologically to Subunit IA. Subunit ID (117.3–136.3 m sub-bottom) is a clayey diatom ooze, characterized by up to 60% diatoms. The lowest subunit (Subunit IE), extending from 136.3 to 155.3 m sub-bottom, is similar to Subunit IA.

Sedimentation rates are unusually high for the Pleistocene and late Pliocene, averaging 50 m/m.y. No unconformities or abrupt changes in sedimentation rate were encountered.

The heat-flow program operated normally. The temperature data clearly show a linear increase with depth. No temperature reversals were recorded.

BACKGROUND AND OBJECTIVES

Site 580 (target Site NW-5A) lies near the present-day subarctic front (42°N) and the northern margin of the transition zone between the subarctic and subtropical gyres. The transition zone defines the convergence of the Kuroshio and Oyashio currents and is marked by high biological productivity. Because of its location, this site will be the reference point for the modern subarctic/subtropical gyre boundary. This site is thought to be the northernmost limit of the subarctic front during the late Neogene and Quaternary.

Our specific scientific objectives were

1. To obtain a detailed paleoceanographic record in the subtropical/subarctic gyre transition zone for the late Miocene to Recent and, in particular, to document the north-south migration of the frontal zone with time.
2. To determine a midlatitude stratigraphy using paleomagnetism, tephrochronology, and biostratigraphy (chiefly siliceous).
3. To determine the time of onset of significant biosiliceous accumulation for comparison with the more southerly Sites 578 and 579.
4. To determine the timing and nature of the onset of the mid-Pliocene and Pleistocene climatic deterioration.
5. To assess the role of orbital forcing in determining pre-Pleistocene paleoclimatic oscillations.
6. To assess the nature and history of authigenic sedimentation in pre-biosiliceous (older than mid-Miocene) sediments.
7. To determine the Cenozoic history of eolian sedimentation for comparison with sites to the south and east.

OPERATIONS

From Site 579, we steamed northward for approximately 1 day, toward Site 580 (target Site NW-5A). Good quality 3.5- and 12-kHz records were collected while underway. The vessel entered the region of NW-5A at approximately 1400 hr. local time (0300Z). Because of the hummocky nature of the bottom topography and because of uncertainties concerning the nature of the to-

¹ Heath, G. R., Burckle, L. H., et al., *Init. Repts. DSDP*, 86: Washington (U.S. Govt. Printing Office).

² Addresses: G. Ross Heath (Co-Chief Scientist) School of Oceanography, Oregon State University, Corvallis, OR 97331 (present address: College of Ocean and Fishery Sciences, University of Washington, Seattle, WA 98195); Lloyd H. Burckle (Co-Chief Scientist) Lamont-Doherty Geological Observatory, Palisades, NY 10964; Anthony E. D'Agostino, ARCO Exploration Company, Houston, TX 77056; Ulrich Bleil, Institut für Geophysik, Ruhr-Universität Bochum, D-4630 Bochum Querenburg, Federal Republic of Germany; Ki-iti Horai, Lamont-Doherty Geological Observatory, Palisades, NY 10964 (present address: Meteorological College, Chiba University, Chiba 277, Japan); Robert D. Jacobi, Department of Geological Sciences, SUNY Buffalo, Amherst, NY 14226; Tom Janecek, Department of Atmospheric & Oceanic Science, University of Michigan, Ann Arbor, MI 48109 (present address: Lamont-Doherty Geological Observatory, Palisades, NY 10964); Itaru Koizumi, College of General Education, Osaka University, Osaka 560, Japan; Lawrence A. Krissiek, School of Oceanography, Oregon State University, Corvallis, OR 97331 (present address: Department of Geology and Mineralogy, Ohio State University, Columbus, OH 43210); Nicole Lenôtre, Bureau de Recherches Géologiques et Minières, Centre Océanologique de Bretagne, 45060 Orléans Cedex, France; Simonetta Monechi, Geological Research Division, Scripps Institution of Oceanography, La Jolla, CA 92093 (present address: Dipartimento di Scienze della Terra, Università di Firenze, 4 Via La Pira, 50121 Firenze, Italy); Joseph J. Morley, Lamont-Doherty Geological Observatory, Palisades, NY 10964; Peter Schultheiss, Institute of Oceanographic Sciences, Surrey GU8 5UB, United Kingdom; Audrey A. Wright, Deep Sea Drilling Project, Scripps Institution of Oceanography, La Jolla, CA 92093 (present address: Ocean Drilling Program, 500 University Drive West, Texas A&M University, College Station, TX 77843).

pography at the target site, the core site was selected some 6 miles short of our target where our air-gun records indicated a reasonably smooth bottom. The beacon was dropped at 1436 local time (0336Z) and gear was retrieved as the vessel passed over the site. At 1630 hr. (0530Z) drill pipe run-in began but was halted at 2130 hr. (1030Z) when the drawworks shorted out. Troubleshooting indicated a problem with a faulty brush holder, which was replaced by 2400 hr. (1300Z). Running in hole continued until 1104 hr. (0004Z), when the corer reached bottom and spudding was attempted. This proved unsuccessful, as the first core recovered only water, and a second attempt was made. This was successful and the first core was recovered shortly thereafter. Following these initial mishaps, the station was occupied without any further problems. Unusually calm seas insured almost complete recovery and relatively little sediment disturbance. The heat-flow shoe was run seven times, all successful. Unfortunately, a combination heat-flow shoe-heat-flow probe-pore water-pressure measurement test failed when a tubing connector on line to the lower pressure port leaked while running in hole. The system was flooded.

A total depth of 155.3 m was reached in one hole at this site. Seventeen cores were recovered, most with full, or close to full, penetration (Table 1).

We departed the site at 0700Z, 7 May, steaming north toward Site 581 (target Site MSS-82C).

LITHOSTRATIGRAPHY

The lithostratigraphy of sediments recovered at Site 580 is based on macroscopic descriptions of the cores and on smear slide analyses with a petrographic microscope. The sediments cored at Site 580 are similar to those cored at Site 579.

The sediments recovered at Site 580 are relatively uniform in color, ranging from gray (5Y 5/1) and dark gray (5Y 4/1) to olive gray (5Y 4/2-5Y 5/2). Smear slide analyses indicate that downhole abundances of siliceous microfossils range from 10 to 70%, averaging about 30%. Quartz abundances average 5%, but range up to 15%. A large number of thin, stiff to indurated, dark greenish gray (5GY 4/1 or 5G 4/1) layers are observed throughout the hole. Smear slide analyses of these layers indi-

cates that they are composed of the same material as the adjacent sediment. Dark gray to black (5Y 3/1, 5Y 3/2, and 5Y 2/1) layers of clay are commonly found immediately below the indurated greenish-gray layers. Volcanic ash layers are common throughout the hole. A total of 89 volcanic ash layers, ranging in thickness from 0.5 to 18.5 cm, were identified (Fig. 1).

Unit I: Siliceous Clay

On the basis of these data, the sedimentary section recovered at Site 580 is classified as a single siliceous clay unit (lithologic Unit I). However, this siliceous clay unit can be subdivided into five subunits (Fig. 1, Table 2).

Subunit IA

This subunit occurs in Cores 1 through 7 and is a siliceous clay containing 2-25% diatoms, 0-15% radiolarians, and 3-15% quartz, with an average composition of approximately 20% diatoms, 10% radiolarians, and 7% quartz. Feldspar and heavy minerals are present in abundances of less than 2%. Volcanic glass contents outside of recognizable ash layers range from 2 to 10%, but are generally greater than 5%. The remainder of the sediment, averaging approximately 56%, is clay material. This subunit contains 43 identifiable ash layers.

Subunit IB

This subunit occurs in Cores 8 and 9, and is a calcareous siliceous clay characterized by 3-25% unspecified clay-sized carbonate material, 10-25% diatoms, 5-7% radiolarians, and 5-10% quartz. Average composition is approximately 10-15% carbonate, 17% diatoms, 6% radiolarians, and 7% quartz. Feldspar abundances are less than 2%, and dispersed ash contents range from 3 to 7%. The remainder of the sediment, averaging approximately 55%, is clay. This subunit contains seven identifiable ash layers.

Subunit IC

This subunit occurs in Cores 10 through 13, and is a siliceous clay similar to Subunit IA. Maximum diatom abundance in Subunit IC is 35%, slightly greater than in Subunit IA, but the approximate average composition of Subunit IC (20% diatoms, 7% radiolarians, 6% quartz) is very similar to that of Subunit IA. Eighteen recognizable ash layers occur in this subunit.

Subunit ID

This subunit occurs in Cores 14 and 15 and is a clayey diatom ooze containing 50-60% diatoms, 2-10% radiolarians, and 5-10% quartz. Average composition of this interval is approximately 52% diatoms, 6% radiolarians, and 7% quartz. Feldspar abundances are a constant 2% throughout this subunit, and dispersed volcanic ash abundances range from 5 to 10%. The remainder of the sediment, averaging approximately 27%, is clay. This subunit contains seven ash layers.

Subunit IE

This subunit occurs in Cores 16 and 17 and is another siliceous clay subunit. It is slightly enriched in siliceous microfossils relative to Subunits IA and IC, with an av-

Table 1. Site 580 coring summary.

Core	Date (June 1982)	Local time	Depth from drill floor (m)	Depth below seafloor (m)	Length cored (m)	Length recovered (m)	Percent recovered
1	6	1428	5386.7-5390.0	0.0-3.3	3.3	3.32	101
2	6	1639	5390.0-5399.5	3.3-12.8	9.5	8.39	88
3	6	1855	5399.5-5409.0	12.8-22.3	9.5	8.62	91
4	6	2105	5409.0-5418.5	22.3-31.8	9.5	8.88	93
5	6	2334	5418.5-5428.0	31.8-41.3	9.5	9.14	96
6	7	0204	5428.0-5437.5	41.3-50.8	9.5	8.80	93
7	7	0440	5437.5-5447.0	50.8-60.3	9.5	7.74	81
8	7	0720	5447.0-5456.5	60.3-69.8	9.5	9.27	98
9	7	0945	5456.5-5466.0	69.8-79.3	9.5	7.51	79
10	7	1200	5466.0-5475.5	79.3-88.8	9.5	8.65	91
11	7	1425	5475.5-5485.0	88.8-98.3	9.5	7.30	77
12	7	1640	5485.0-5494.5	98.3-107.8	9.5	9.29	98
13	7	1850	5494.5-5504.0	107.8-117.3	9.5	9.08	96
14	7	2117	5504.0-5513.5	117.3-126.8	9.5	9.14	96
15	8	0330	5513.5-5523.0	126.8-136.3	9.5	8.45	89
16	8	0620	5523.0-5532.5	136.3-145.8	9.5	8.97	94
17	8	0902	5532.5-5542.0	145.8-155.3	9.5	7.72	81
					155.3 (total)	140.74 (total)	91 (avg.)

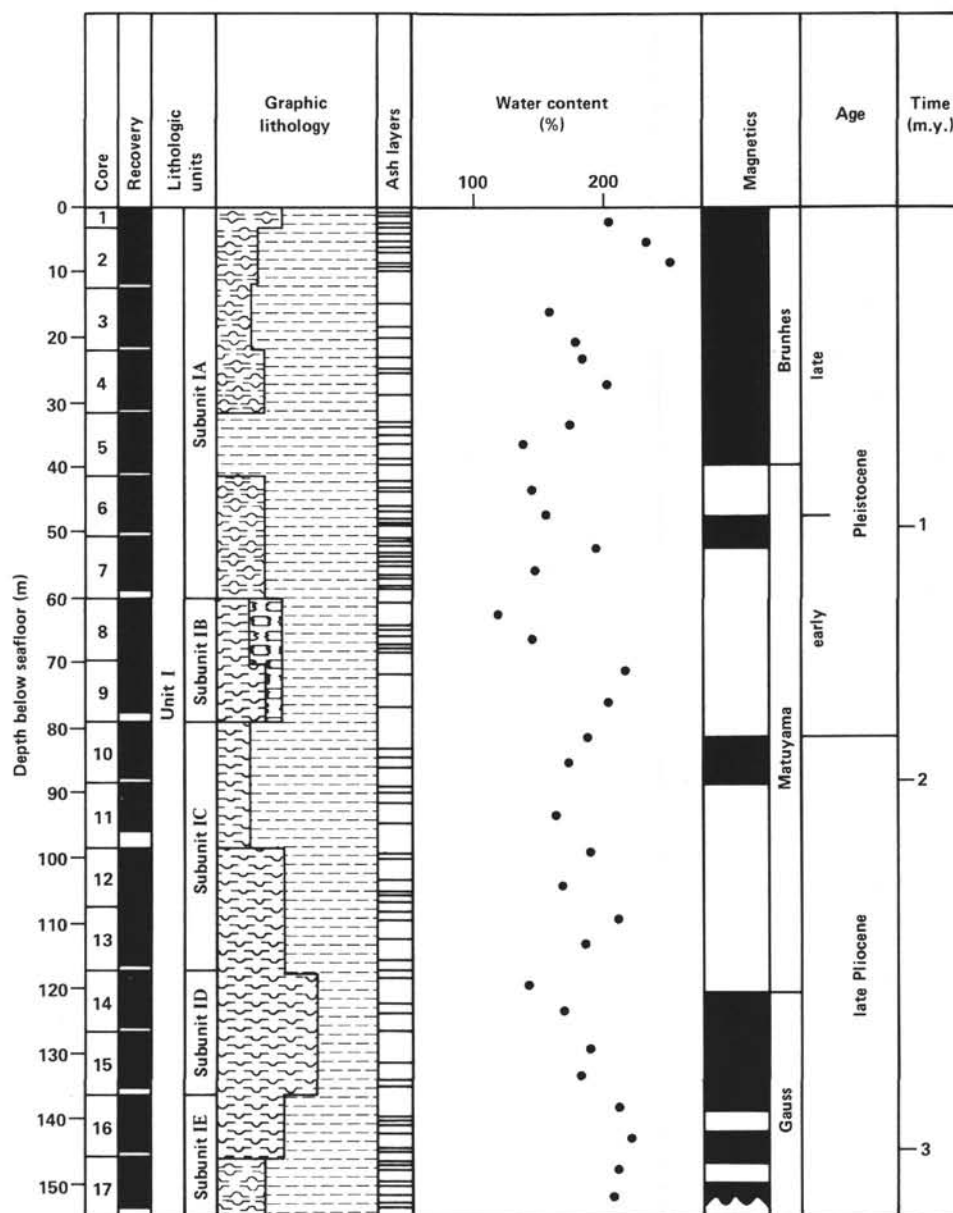


Figure 1. Site summary diagram showing Site 580 core numbers, core recovery, lithologic units, graphic lithology, ash layer locations, water content (%), magnetostratigraphy, and age. Symbols used in graphic lithology column are defined in Introduction and Explanatory Notes (this volume).

Table 2. Site 580 lithostratigraphic units.

Lithologic unit	Cored interval	Sub-bottom depth (m)
I: Siliceous clay		
Subunit IA: siliceous clay	1-1, 0 cm to 7,CC	0.0-60.3
Subunit IB: calcareous siliceous clay	8-1, 0 cm to 9,CC	60.3-79.3
Subunit IC: siliceous clay	10-1, 0 cm to 13,CC	79.3-117.3
Subunit ID: clayey diatom ooze	14-1, 0 cm to 15,CC	117.3-136.3
Subunit IE: siliceous clay	16-1, 0 cm to 17,CC	136.3-155.3

erage composition of approximately 27% diatoms and 8% radiolarians. Feldspar is rare to absent, quartz averages 7%, and dispersed volcanic glass abundances range from 2 to 10%, averaging approximately 5%. The re-

mainder of the sediment, averaging approximately 53%, is clay. This subunit contains 14 recognizable ash layers.

SEISMIC CORRELATION

High-resolution seismic reflection profiles (3.5 and 12 kHz) and 100-Hz reflection profiles were recorded at Site 580. Only a hull-mounted 3.5-kHz sound source was utilized. The 3.5-kHz echograms over Site 580 reveal a fairly uniform seismic section of parallel sub-bottom reflectors (Fig. 2). This seismic section can be divided into a four-part sequence based on gaps in the reflector sequence and relative strength of the return signals (Table 3).

The uppermost seismic unit consists of three strong reflectors and extends to 0.0166 s below the seafloor

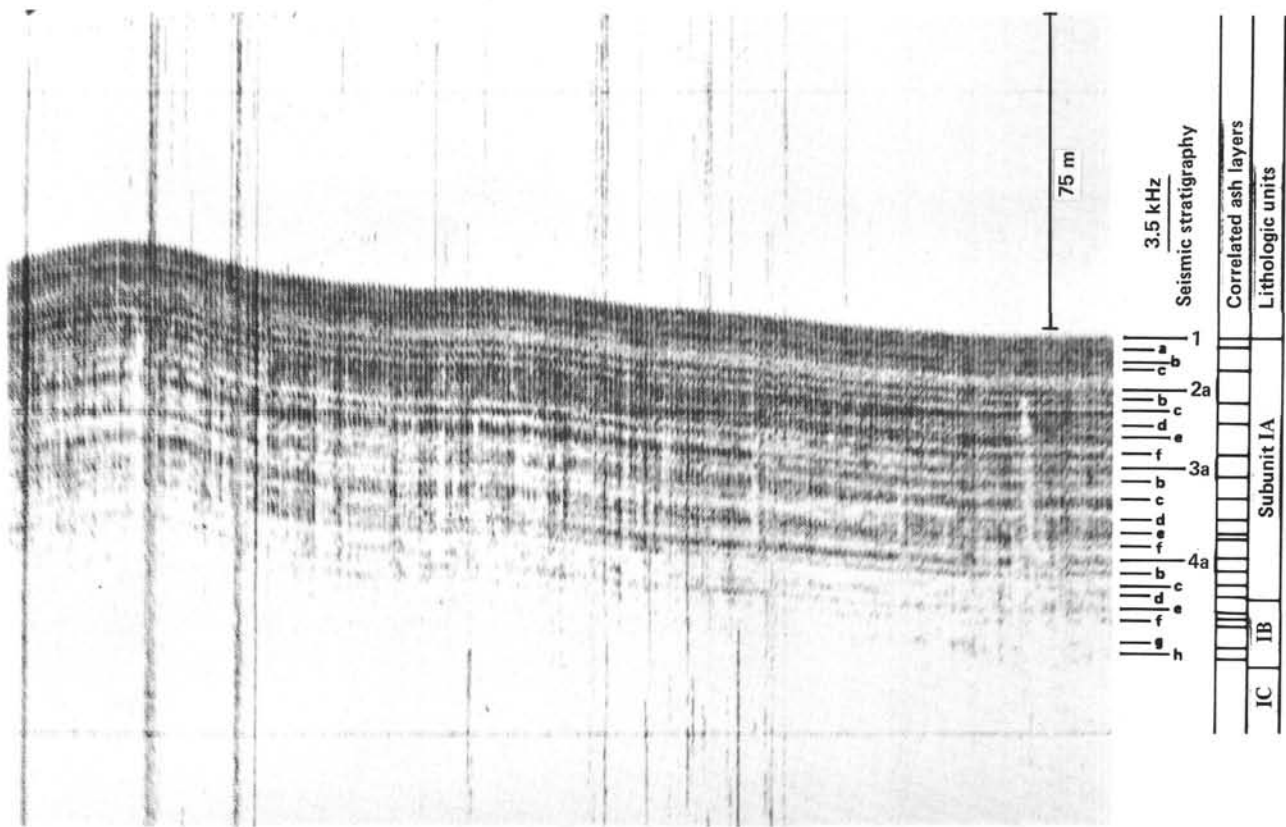


Figure 2. 3.5-kHz echogram near Site 580 showing the four-part seismic sequence described in the text. Sub-bottom depths and sources of seismic reflectors are given in Table 3.

Table 3. 3.5-kHz seismic correlations, Site 580.

Reflector	Relative strength ^a	Sub-bottom depth (s)	Sub-bottom depth (m)			Source		
			1440 m/s	1480 m/s	1504 m/s	Depth (m)	Lithology	Thickness (cm)
1a	S	0.00269	1.94	1.99	2.02	2.25	Ash 2	10.5
b	S	0.00662	4.76	4.90	4.98			
c	S	0.0108	7.78	7.96	8.12	7.7	Ash 8	15
2a	S	0.0166	11.95	12.24	12.48		No core	
b	S	0.0200	14.4	14.77	15.04	15.34	Ash 11,12	6,6
c	S	0.0228	16.42	16.836	17.15			
d	S	0.0269	19.39	19.90	20.23	19.8	Ash 16	2
e	S	0.0310	22.32	22.96	23.3	24.6	Ash 18?	6
f	S	0.0362	26.06	26.78	27.22	27.8	Ash 19?	6
3a	I	0.0413	29.74	30.53	31.06			
b	I	0.0447	32.18	33.06	33.61	32.8	Ash 20	8
c	I	0.0506	36.43	37.42	38.05			
d	IT-I	0.0568	40.90	42.01	42.71	42.75	Ash 27	14
						42.8	Ash 28	9
e	W-I	0.0612	44.06	45.30	46.02	45.45	Ash 32?	5
						46.4	Ash 33?	16
f	W	0.0642	46.22	47.52	48.28	47.25	Ash 35	5
4a	W-I	0.0685	49.32	50.66	51.51	51.6	Ash 37	11
b	IT-I	0.0724-	52.13-	53.57-	54.44-	54.3	Ash 42	13
		0.0732	52.70	54.18	55.05			
c	IT	0.0765	55.08	56.63	57.53	57.7	Ash 46	3
d	IT-W	0.0796-	57.31-	58.92-	59.86-	60.4	Ash 49	6
		0.0807	58.10	59.69	60.69			
e	IT-W	0.0839-	60.41-	62.06-	63.09-	64.0	Ash 50	6
		0.0848	61.06	62.75	63.77			
f	IT-W	0.0888	63.94	65.66	66.78	65.6	Ash 52	13
						67.5	Ash 53?	5
g	IT	0.0954	68.69	70.63	71.74	72.2	Ash 56	11
h	IT	0.0998	71.86	73.88	75.05	75.8	Ash 57	9

^a S = strong; I = Intermediate; IT = intermittent, but weak; W = weak, but generally continuous.

(12.5 m at 1504 m/s). A thin transparent layer below the deepest reflector in seismic Unit 1 separates that unit from the top of seismic Unit 2. Seismic Unit 2 consists of six strong reflectors and extends to 0.413 s below the seafloor (31.1 m at 1504 m/s). A very thin transparent layer at the base of seismic Unit 2 separates that unit from the top of seismic Unit 3. Seismic Unit 3 consists of six reflectors of variable strengths and extends to 0.0685 s below the seafloor (51.5 m at 1504 m/s). Seismic Unit 4 consists of generally weak and discontinuous reflectors; only the top reflector is of intermediate strength. Unit 4 extends to 0.0998 s below the seafloor (75.0 m at 1504 m/s).

The source of these reflectors was difficult to determine primarily because of the large number of close equally spaced ash layers and indurated clay layers. In general, the reflectors correlate with ash layers, especially below about 45 m sub-bottom depth (Fig. 2, Table 3). However, several strong reflectors in the upper 45 m correlate with sections of core that do not contain ash layers. These strong reflectors could result from interference effects due to the ubiquitous thin, indurated pyritic clay layers. Alternatively, ash layers displaced in the core by unrecognized zones of "flow-in" or ash layers assigned incorrect depths because of inaccurate depth to the top of the core could account for the reflectors. The top of lithostratigraphic Subunit IB (60.3 m sub-bottom) is near Reflector 4d (~59.8–60.7 m, Table 3).

The 100-Hz seismic reflection profiles reveal a four-part seismic section at Site 580 (Fig. 3). The uppermost seismic unit (Unit 1) extends to 0.295 s below the seafloor (221 m at 1500 m/s) and consists of four subunits. The uppermost seismic subunit (1a) is composed of strong, parallel, and continuous reflectors. Subunit 1a extends to 0.01 s below the seafloor (75 m at 1500 m/s), corresponds with the entire 3.5-kHz seismic section (Fig. 2, seismic Units 1, 2, 3, and 4), and correlates with lithostratigraphic Units IA, IB, and perhaps the very top of IC. Seismic Subunit 1b occurs between 0.01 and 0.195 s (146.2 m at 1500 m/s) and is a zone of weak, discontinuous reflectors that wedge out away from the site. It correlates with lithostratigraphic Units IC and ID. Seismic Subunit 1c extends to 0.22 s below the seafloor (165 m at 1500 m/s) and consists of strong, continuous, and parallel reflectors. It may correlate with lithostratigraphic Subunit IE. Seismic Subunit 1d extends to 0.295 s below the seafloor (221.2 m at 1500 m/s) and is a transparent layer.

Seismic Unit 2 is divided into two subunits. Seismic Subunit 2a consists of strong, continuous, parallel reflectors extending to about 0.36 s below the seafloor (270 m at 1500 m/s). Seismic Subunit 2b is a transparent zone extending to 0.50 s below the seafloor (375 m at 1500 m/s).

Seismic Unit 3 consists of strong, slightly incoherent echoes that extend to 0.57 s below the seafloor. Seismic

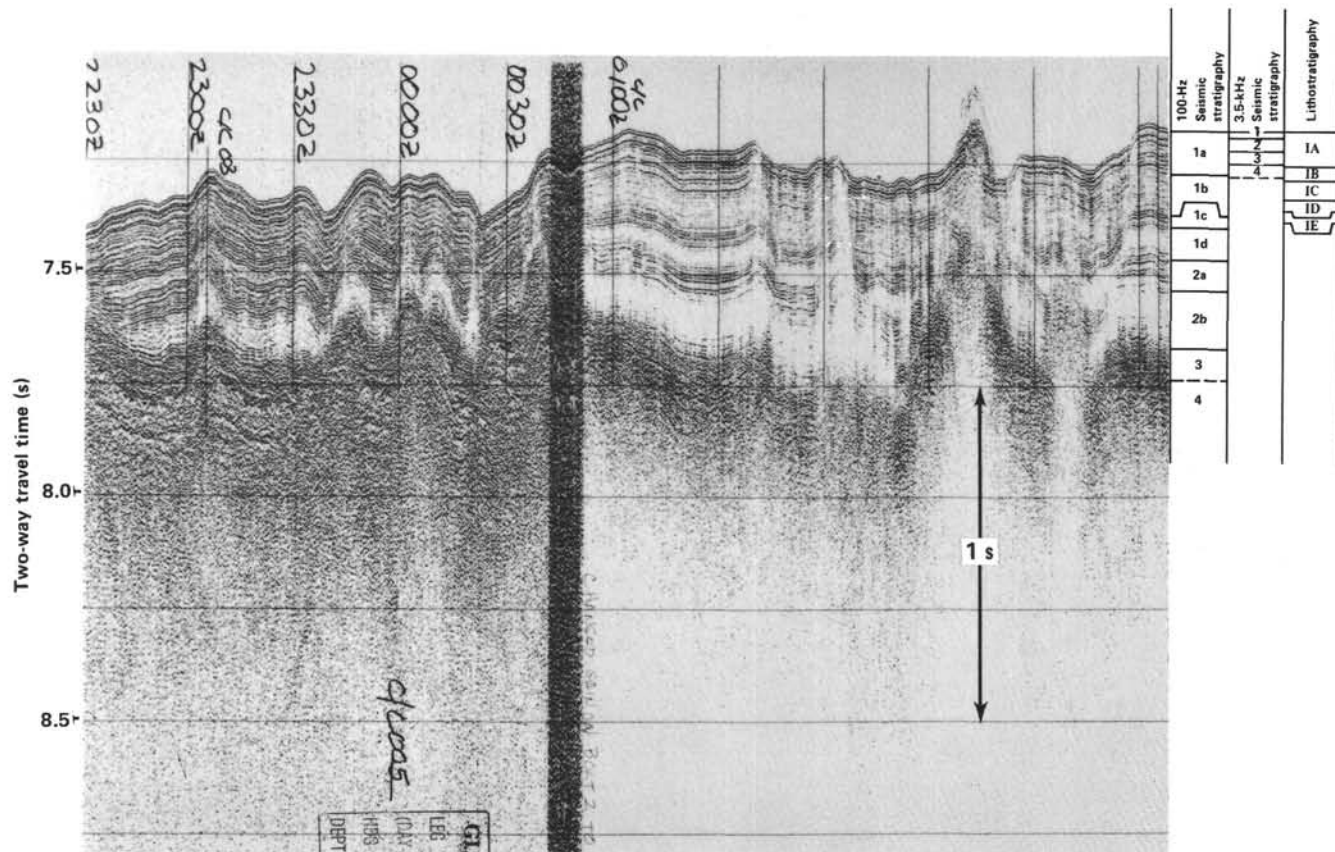


Figure 3. 100-Hz reflection profile over Site 580 showing the four-part seismic sequence described in the text and correlative 3.5-kHz seismic stratigraphic units and lithostratigraphic units.

Unit 3 is conformable with seismic Unit 4 underlying it, but unconformable with the overlying seismic units; both seismic Units 1 and 2 downlap Unit 3 over bathymetric highs. The source of seismic Units 2b and 3 is equivocal but based on the unconformity, the echo character, and the sub-bottom depth, it is probable that seismic Unit 2b is pelagic clay and seismic Unit 3 is Cretaceous chert and associated sedimentary rocks.

Seismic Unit 4 consists of a strong, slightly prolonged reflector and probably is basaltic "basement."

BIOSTRATIGRAPHY

About 155 m of Quaternary and late Pliocene sediments were recovered at Site 580. Abundant, well-preserved diatoms were found in all samples examined. Radiolarians were also common to abundant and well preserved in most sections. Rare to common silicoflagellates were noted in all core-catcher samples. In four core-catcher samples, poorly to moderately preserved foraminifers were recovered. Common, poorly preserved calcareous nannofossils were found in one core-catcher sample (580-13,CC).

The biostratigraphic summary based on three groups of microfossils is shown in Figure 4. The boundary between early and late Pleistocene occurs near the base of Core 6, and the Plio-Pleistocene boundary falls near the top of Core 11 based on the radiolarian and diatom biostratigraphic data.

Calcareous Nannofossils

Only one sample (580-13,CC) contained calcareous nannofossils. The poorly preserved assemblage includes *Crenolithus daronicoides*, *Coccolithus pelagicus*, *Calcidiscus macintyreii*, *Cyclococcolithus leptoporus*, *Emiliana ovata*, *Ceratolithus rugosus*, *Discoaster brouweri*, and *Reticulofenestra* sp. This assemblage indicates a probable Pliocene age.

Foraminifers

Core-catcher samples from all 17 cores recovered at Hole 580 were examined. Four core-catcher samples contained foraminifers (580-1,CC; 580-2,CC; 580-5,CC; 580-13,CC). Samples 580-1,CC, 580-2,CC, and 580-5,CC contained a Pleistocene assemblage typical of the *Glo-*

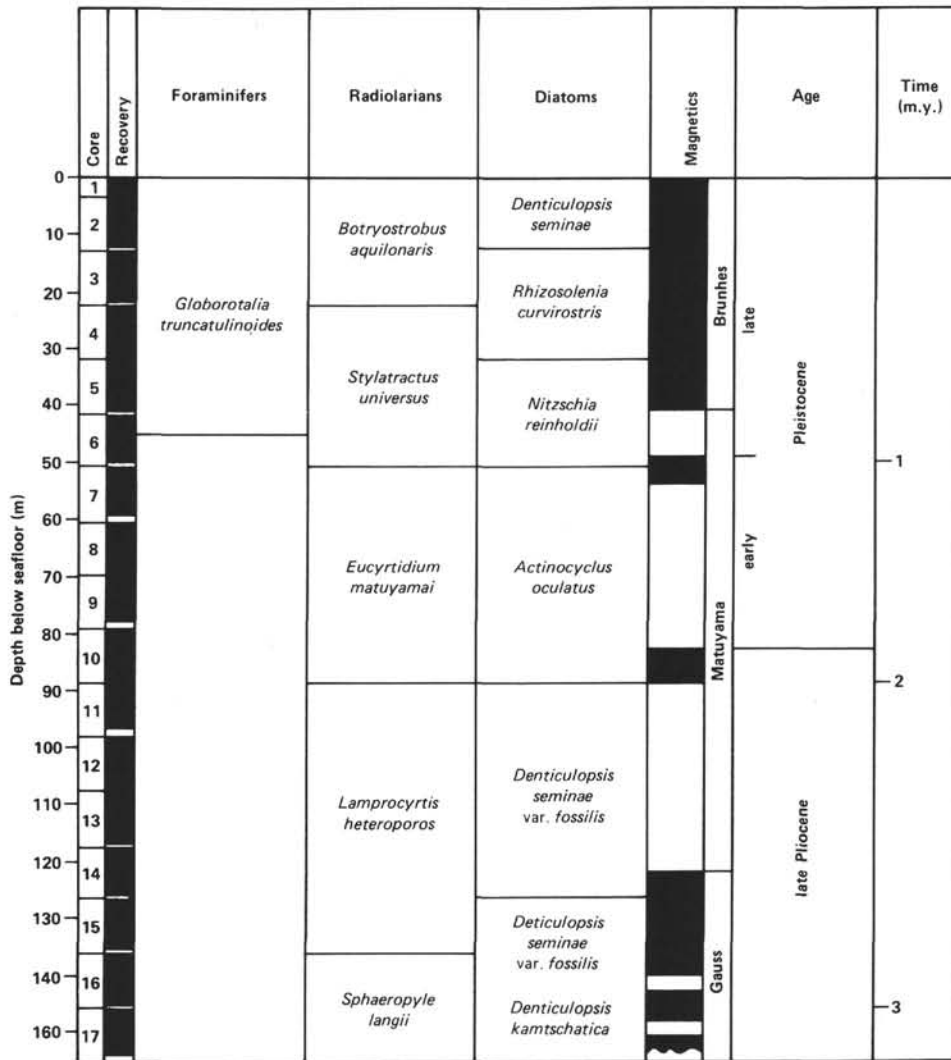


Figure 4. Site 580 biostratigraphic and magnetostratigraphic summary.

borotalia truncatulinoides Zone (Stainforth et al., 1975) or Zone N22 (Blow, 1969). The fauna included *G. truncatulinoides* (580-1, CC only), *G. humerosa*, *G. acostaensis*, *G. continua*, *G. obesa*, *G. inflata*, and *Neogloboquadrina pachyderma* (sinistral). Samples 580-1, CC and 580-2, CC contain rare benthic species such as *Pullenia quinqueloba*, *Cibicides pseudoungerianus*, *Melonis affinis*, *M. pompilioides*, *Gyroidina neosoldanii*, and *Parafissurina* spp. Shore-based studies have shown that this Pleistocene planktonic fauna can be found as deep as 44.9 m (Sample 580-6-3, 60 cm). Sample 580-13, CC contained an upper Pliocene fauna indicative of the upper part of the *Pulleniatina obliquiloculata* Zone equivalent to N21. The fauna consists of *Globorotalia humerosa*, *G. acostaensis*, *G. obesa*, *G. venezuelana*, *G. crassaformis*, and *Pulleniatina primalis*.

Preservation of all the specimens was poor to moderate. All show heavy but uniform dissolution effects. The tests are fragile and appear chalky. Features such as pores and apertures are commonly enlarged. Where present, the abundance of foraminifers in Hole 580 was low with only about 30–50 specimens per 10–15 cm³ sample.

Radiolarians

Sediment samples from Hole 580 contain late Quaternary through late Pliocene radiolarians. Figure 4 shows the shipboard radiolarian biostratigraphy for this site.

All core-catcher samples from Hole 580 contain radiolarians. Common, well-preserved radiolarians characteristic of the late Pleistocene *Botryostrobus aquilonaris* Zone (Hays, 1970) are found in Samples 580-1, CC through 580-3, CC. Samples 580-4, CC through 580-6, CC contain generally well-preserved common to abundant radiolarians. The presence of *Stylatractus universus* and the absence of *Eucyrtidium matuyamai* in these cores (Cores 4 through 6) indicate that this sediment sequence belongs to the *S. universus* Zone (Hays, 1970). The *E. matuyamai* Zone (Hays, 1970; Foreman, 1973) is represented in sediment from this hole in Samples 580-7, CC through 580-10, CC based on the presence of the radiolarian species *E. matuyamai*. The sediment sequence in Samples 580-11, CC through 580-15, CC is assigned to the *Lamprocyrtis heteroporos* Zone (Hays, 1970; Foreman, 1975) based on the absence of *E. matuyamai* and *Stichocorys peregrina*. The radiolarians found in Samples 580-16, CC and 580-17, CC are late Pliocene in age, based on the presence of *S. peregrina*. The faunal assemblage in these cores (Cores 16 and 17) is characteristic of the mid to upper portion of the *Sphaeropyle langii* Zone (Foreman, 1975) since *Lamprocyrtis heteroporos* in addition to *Stichocorys peregrina* is present in these sediment samples.

Diatoms

A thick Quaternary and late Pliocene diatom biostratigraphic section was recovered at Site 580 and is suitable, in conjunction with Site 579, for a study of north-south migrations of the cold-water Oyashio Current and the warm-water Kuroshio Current from late Pliocene to Recent time. As cold-water species are dominant, the dia-

tom zonation of Koizumi (1973) is applied to this section. Diatoms are abundant and well preserved.

Cores 1 and 2 belong to the latest Quaternary *Denticulopsis seminae* Zone, and Cores 3 and 4 to the late Pleistocene *Rhizosolenia curvirostris* Zone. Cores 5 and 6 are assigned to the middle Pleistocene *Nitzschia reinholdii* Zone. The last occurrence of the silicoflagellate *Mesocena quadrangula*, which is around the Jaramillo Event of the geomagnetic Matuyama Epoch, occurs in Core 6. The early Pleistocene *Actinocyclus oculatus* Zone occurs in samples from Cores 7 to 10. The Pliocene/Pleistocene boundary is placed between *Coscinodiscus pustulatus* and *Thalassiosira zabelina* in Core 11. Cores 11 through 14 are assigned to the late Pliocene *D. seminae* var. *fossilis* Zone by the presence of *D. seminae* var. *fossilis* and the absence of *D. kamtschatica*. Core 13 is placed in the lower Matuyama Epoch between the Olduvai Event and the top of the Gauss Epoch by the presence of *Thalassiosira convexa* and the absence of *D. kamtschatica*. Diatom assemblages in Cores 15 through 17 are placed in the *D. seminae* var. *fossilis*-*D. kamtschatica* Zone. Core 17 is estimated to be more than 2.7 m.y. old because of the presence of *N. jouseae*.

PALEOMAGNETICS

Paleomagnetic analyses using stepwise alternating field (AF) demagnetization techniques were made on 358 samples from the 155.3 m of sediments penetrated at Site 580.

In the upper part of the hole, the intensities of the natural remanent magnetization (NRM) show a systematic overall decrease from about 6×10^{-5} Gauss near the top of the hole to about 6×10^{-7} Gauss at about 120 m sub-bottom. Below this level, to the base of the hole, NRM intensities were somewhat higher again. With virtually all the cores, NRM values vary by at least one order of magnitude. In contrast, the magnetic stability remains remarkably constant throughout. Median destructive field (MDF) measurements typically fall within the range of 300 ± 50 Oe. The directional changes between NRM and stable directions upon AF demagnetization are generally small.

The polarity pattern derived from the downhole variation of the stable magnetization directions is shown in Figure 4. The Brunhes/Matuyama boundary was identified at 40.00 m sub-bottom (Sample 580-5-6, 70 cm), and the Matuyama/Gauss boundary at 121.44 m sub-bottom (Sample 580-14-3, 114 cm). The Jaramillo and Olduvai events in the reversed Matuyama Epoch as well as the Kaena and Mammoth events in the normal Gauss Epoch are clearly recognizable in the record. In addition, one of the short events of the Reunion series and a yet unnamed event between the Jaramillo and Olduvai were found. The base of the hole, at 155.30 m sub-bottom, did not reach the Gauss/Gilbert boundary. Using the most recent polarity time scale of Berggren et al. (in press), the extrapolated absolute age at the base of the hole is about 3.30 m.y. The sediment column at this site accumulated at a remarkably constant average rate of about 46.5 m/m.y.

Above a sub-bottom depth of about 120 m (corresponding roughly to the Matuyama/Gauss boundary at 2.47 m.y.), the stable inclinations measured scatter around the axial dipole value for the present latitude of the site (60.6°). Only below this depth does the stable inclination record gradually become shallower, reflecting the northward component of the Pacific Plate motion.

The general variation in the inclination data throughout the hole apparently results from a normal range of secular paleofield variation. In contrast, the stable declination pattern is much more complex as it frequently includes variable amounts of disturbances introduced by the coring process.

SEDIMENT ACCUMULATION RATES

Nine radiolarian and diatom biostratigraphic zonal boundaries identified in the cores of Site 580 (Fig. 4), in addition to the paleomagnetic stratigraphy, were used to estimate the sediment accumulation rates at this site. The resulting curve (Fig. 5) shows a remarkably constant rate of deposition of almost 50 m/m.y. for the Quaternary through late Pliocene.

PHYSICAL PROPERTIES

Physical properties measurements at Site 580 were performed using mainly standard Deep Sea Drilling Project (DSDP) methods (Boyce, 1976a,b; see Introduction and Explanatory Notes, this volume). Table 4 summarizes the properties that were measured in Hole 580. These measurements were generally taken at 4.5-m intervals throughout the core. Detailed compressional wave velocity profiles were made on selected ash layers to determine the fine-scale velocity structure. Figures 6, 7, and 8 show profiles of compressional wave velocity, saturated bulk density and water content, and shear strength, respectively.

A full discussion of the physical properties of the recovered sediment, including tables of the data, is given by Schultheiss (this volume). Some of the more interesting features of the data are highlighted here:

1. As at Sites 578 and 579, the velocity profile for Site 580 (Fig. 6) is dominated by high velocity pyrite-in-durated clay and ash beds. Velocities in the siliceous clays and oozes rise gradually downhole from about 1470 m/s

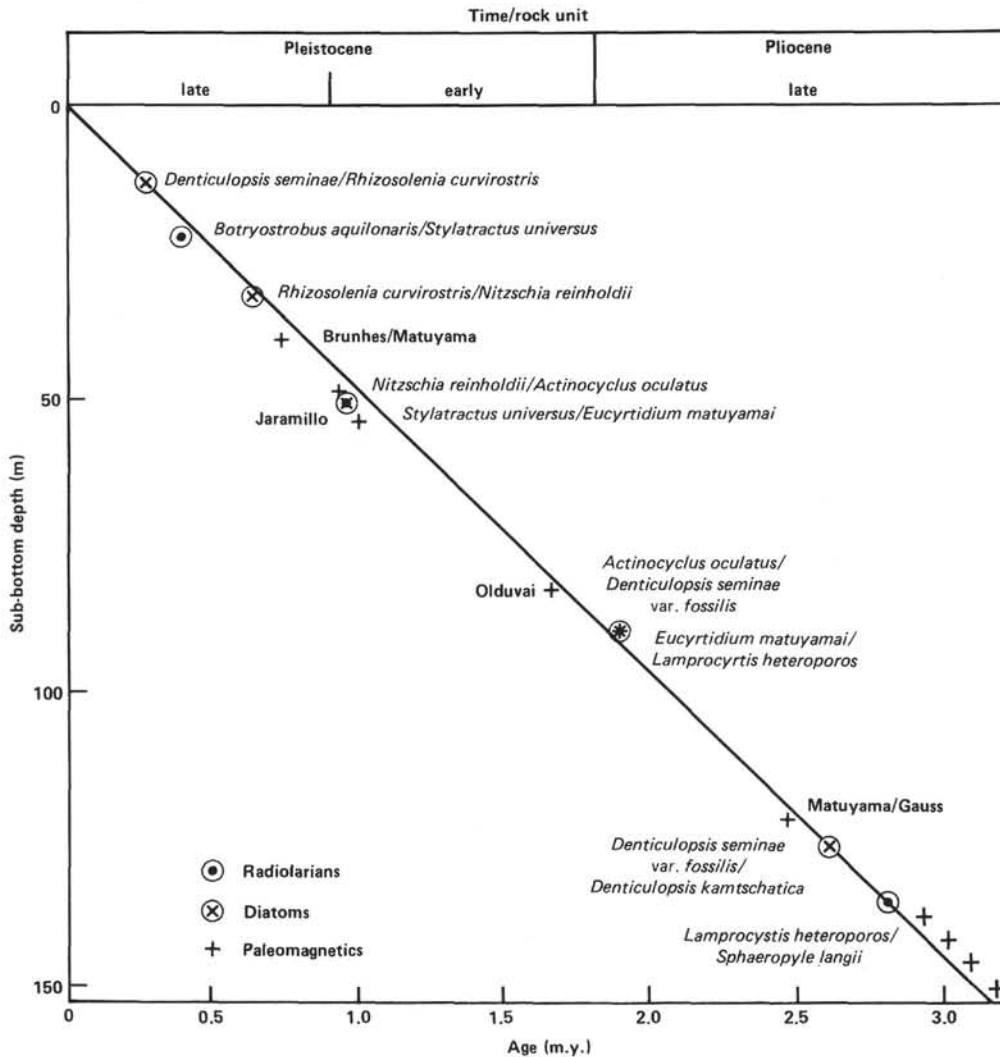


Figure 5. Site 580 sediment accumulation rates.

Table 4. Physical properties measurements made at Site 580.

Hole 580	
Shear strength	
Hand-operated vane	x
Motorized vane	x
Compressional wave velocity	x
Water content/bulk density	
Shipboard analysis	x
Shore-based analysis	x
Bulk density by 2-min. GRAPE	x

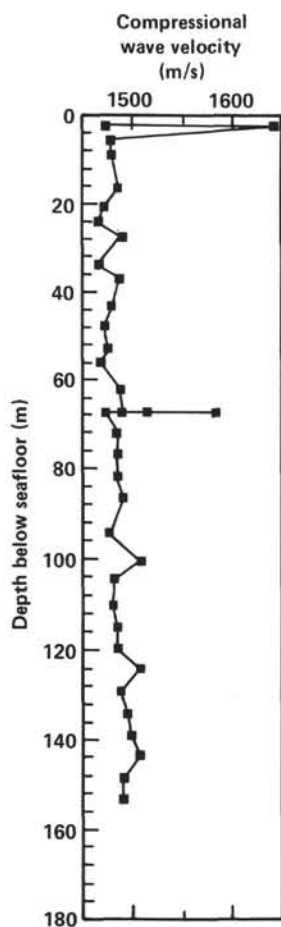


Figure 6. Plot of compressional wave velocity versus sub-bottom depth at Site 580.

in Core 1 to 1490 m/s in Core 17 at a sub-bottom depth of 150 m.

2. A detailed velocity structure was obtained from five ash layers by taking measurements at 1 or 2 cm intervals through the beds. Some of these examples clearly showed that the sharp basal contact produced a maximum velocity near or at the bottom of the ash layer. The velocities tend to decrease more slowly up through the layers.

3. The velocity structure in these ash beds is primarily governed by their bulk density structure. A comparison of the GRAPE record with the measured velocity profile for Section 580-2-2 illustrated the close relation-

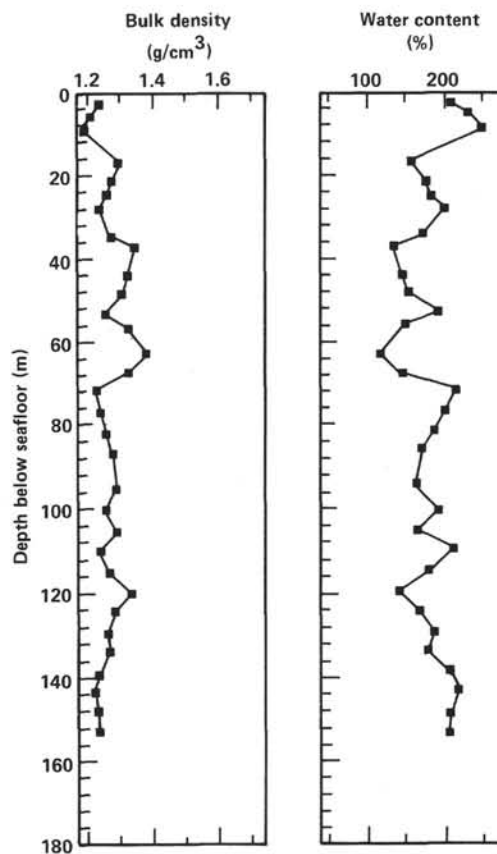


Figure 7. Plot of saturated bulk density and water content versus sub-bottom depth at Site 580.

ship between the two profiles. This type of detailed profile may prove useful for modeling acoustic reflectors for correlation with seismic sections.

4. The water-content profile (Fig. 7) shows an erratic decrease from around 230% at the seafloor to 120% at 63 m sub-bottom. This roughly corresponds to lithologic Subunit IA (siliceous clay). An increase of up to 212% in water content occurs in Subunit IB (calcareous siliceous clay, 60.3–79.3 m). In Subunit IC (79.3–117.3 m), which is lithologically similar to Subunit IA, the water content is essentially constant at about 180%. Lithologic Subunit ID (diatom ooze) initially exhibits a decrease in water content to 140% but then increases slowly through Subunit ID before decreasing again in Subunit IE (which is lithologically similar to IA and IC).

5. The shear strength measurements (Fig. 8) show a nearly linear increase with depth up to 800 g/cm² at 150 m sub-bottom.

INORGANIC GEOCHEMISTRY

Six squeezed core samples from Hole 580 were analyzed for the standard suite of components: pH, alkalinity, salinity, chlorinity, calcium, and magnesium (Table 5). No *in situ* samples were taken.

As at the two prior sites, calcium increases linearly with depth (Fig. 9), suggesting diffusion from a carbonate source beneath the drilled section to the seafloor. Magnesium decreases nonlinearly with depth, probably

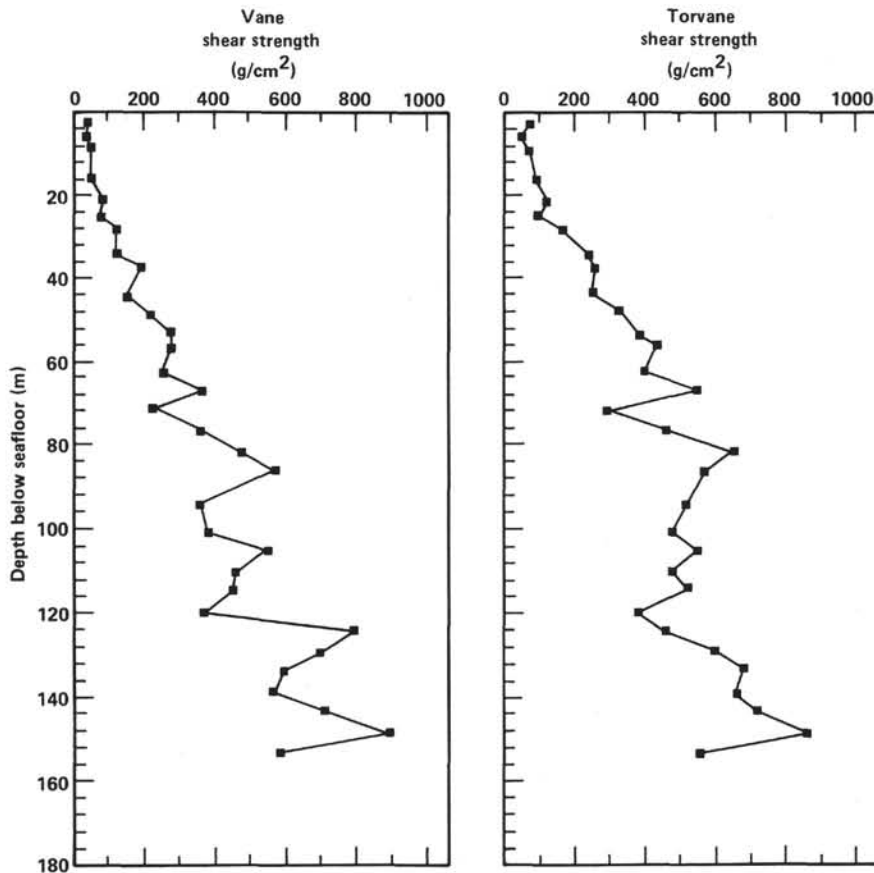


Figure 8. Plot of shear strength versus sub-bottom depth at Site 580.

Table 5. Inorganic geochemistry measurements made at Site 580.

Sample	pH	Alkalinity (mEq/l)	Salinity (‰)	Calcium (mM)	Magnesium (mM)	Chlorinity (‰)
IAPSO	7.81	2.45	35.2	10.55	53.99	19.376
SSW	7.96	2.33	34.1	10.15	51.62	18.58
580-2-5, 140-150 cm	7.61	5.85	35.2	10.61	51.22	19.36
580-5-5, 140-150 cm	7.59	7.87	35.2	11.22	49.12	19.16
580-8-5, 140-150 cm	7.49	8.44	35.2	11.41	47.45	19.39
580-11-4, 140-150 cm	7.55	8.64	34.9	11.79	46.42	19.46
580-14-5, 140-150 cm	7.57	8.59	34.9	12.16	46.04	19.36
580-17-5, 140-150 cm	7.64	8.43	34.9	12.29	45.68	19.36

due to uptake by the abundant altering ash in the drilled section. Alkalinity increases with depth to about 60 m, presumably due to oxidation of organic matter by sulfate-reducing bacteria, which must outweigh the effects of the alteration of volcanic ash.

HEAT FLOW

Measurements of sediment temperature using the new Woods Hole Oceanographic Institution (WHOI) heat-flow instrument were made at 11 locations in Hole 580. All runs were successful. Recorder WHOI-4A, connected either to battery pack NTLT-2 or NTLT-3, was used at every other core starting with Core 3 throughout the hole. At the sub-bottom depth interval of 60 to 100 m, where temperature distributions were most complex at the two previous sites, auxiliary measurements were made by recorder WHOI-01 connected to battery pack TILT-3. A comparison run with the conventional ERI-type heat flow instrument was made using the same recorder-bat-

tery unit. The comparison was unsuccessful owing to a failure on the part of the ERI-type instrument. The data from the new WHOI instrument were, however, useful and are valuable in providing a detailed temperature profile in a relatively shallow sediment section. The temperature data, combined with a detailed thermal conductivity profile constructed from 250 measurements on cores recovered from Hole 580, provided an estimate of heat flow at this site (see Horai and Von Herzen, this volume).

Past DSDP heat-flow studies have measured down-hole temperatures at typical intervals of 100 m in deep holes. Oceanic heat-flow studies from ordinary research vessels have measured near-surface temperature to a depth of 10 to 15 m at intervals of 1 to 2 m. The field tests made on this leg demonstrated that the new WHOI hydraulic piston core (HPC) core-nose heat-flow instrument can be deployed successively to yield detailed temperature profiles in soft oceanic sediments.

SUMMARY AND CONCLUSIONS

At Site 580, we recovered a thick sequence of Quaternary and late Pliocene sediments. Siliceous microfossils (diatoms and radiolarians) are generally abundant and moderately to well preserved. An excellent magnetic reversal record can be identified back to the middle of the Gauss Normal Epoch.

One hundred and fifty-five meters of sediment were penetrated. Except for the numerous ash layers, these

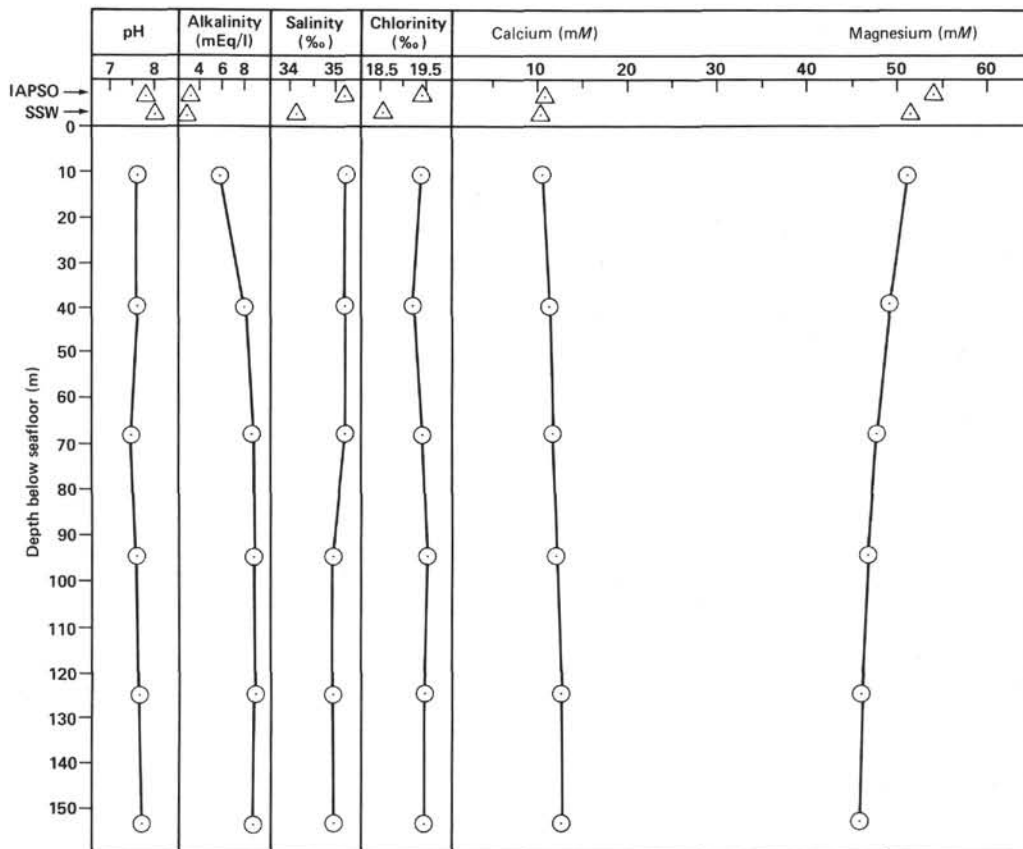


Figure 9. Profiles of pH, alkalinity, salinity (‰), chlorinity (‰), calcium (mM), and magnesium (mM) versus sub-bottom depth for interstitial water samples analyzed at Site 580. Symbols are as follows: Δ = IAPSO and SSW standards; \odot = samples from Hole 580.

sediments are relatively uniform in color and texture. As at Site 579, we encountered numerous thin, well indurated, dark grayish green layers that were lithologically dissimilar from the adjacent, soft biosiliceous clay. Unlike Site 579, thin, dark gray to black layers of clay are commonly found immediately below the indurated layers.

The sediments from this site are placed into one lithologic unit, which is characterized as a siliceous clay, gray to dark gray to olive gray in color, with variable abundances of biogenic silica ranging from 10 to 70%. Based on these discrete changes in lithology and on the unexpected occurrence of clay-sized carbonate in one section of the hole, we can subdivide lithologic Unit I as follows:

Subunit IA (0–60.3 m) is a siliceous clay that is gray, olive gray, to dark gray in color. It contains 2–25% diatoms, 0–15% radiolarians, and 3–15% quartz. Feldspar and heavy minerals are present in abundances of less than 2%, while disseminated ash ranges from 2 to 10% in abundance. The remainder of the sediment (56%) is clay. The subunit contains 43 ash layers.

Subunit IB (60.3–79.3 m) is a calcareous biosiliceous clay. The distinguishing characteristic is the presence of 3 to 25% unspecified clay-sized carbonate. Additionally, the subunit contains 10–25% diatoms, 5–7% radiolarians, and 5–10% quartz. Quartz abundance ranges up to 10%, while feldspar is usually less than 2% and disseminated ash ranges from 3 to 7%. The remainder

of the sediment (55%) is composed of clay. The subunit contains seven recognizable ash layers.

Subunit IC (73.9–117.3 m) is a siliceous clay with average composition similar to that of Subunit IA. Eighteen recognizable ash layers occur in this unit.

Subunit ID (117.3–136.3 m) is a clayey diatom ooze containing 50–60% diatoms, 2–10% radiolarians, and 5–10% quartz. Feldspar abundances are a constant 2% throughout this layer and disseminated ash ranges from 5 to 10%. The remainder of the sediment (~27%) is clay. This subunit contains seven ash layers.

Subunit IE (136.3–155.3 m) is another siliceous clay similar in composition to Subunits IA and IC except that it is slightly more enriched in diatoms. The bulk of the sediment (~53%) is clay. This subunit contains 14 ash layers.

Although the stiff greenish gray layers were present throughout all seventeen cores recovered, their locations were not recorded in the same detail as the ash layers.

Figure 4 summarizes the paleomagnetism and biostratigraphy for this site. Because of good weather, excellent recovery was achieved with minimum flow-in or coring disturbance. Thus, an excellent paleomagnetic reversal record was obtained at this site. Additionally, there was unusually fine preservation of the siliceous microfossils, making it possible to verify the magnetic reversal record via biostratigraphy. Both of the major siliceous microfossil groups (radiolarians and diatoms) were used to

verify that the hole bottomed in the middle part of the Gauss. This excellent stratigraphic control permitted us to determine, in detail, sedimentation rates during the interval of time covered by this hole. Figure 5 is an age-depth curve for the interval sampled. Sedimentation rates are high (on the order of 50 m/m.y.) in the Pleistocene and late Pliocene.

Figure 10 shows the numbers of ash layers accumulated per million year interval. There is a high of 48 ash layers during the late Pleistocene and only 18 during the early Pleistocene and latest Pliocene. This does not conform with the pattern that we saw at Sites 578 and 579 or with what Furuta and Arai (1980) observed at Site 436. Since this site has been well within the range of ash falls during the entire depositional history of this hole, changes in the number of ash layers accumulated per unit time may well represent evidence for episodicity.

Because of the large number of ash layers at this site it was difficult to determine the sources of the seismic reflections. In general, the reflectors correlated with the ash layers below 45 m sub-bottom depth. However, there were several strong reflectors in the upper 45 m that definitely did not correlate with ash layers. It is entirely possible that these strong reflectors may result from the ubiquitous, indurated to semi-indurated gray-green layers. The 100-Hz seismic reflection profiles indicate a four-part seismic section at this site. The uppermost seismic unit (0–221 m at a velocity of 1.5 km/s) includes the interval cored at this site and is subdivided into four subunits. Subunits 1a and 1c contain distinct, continuous reflectors while Subunit 1b contains indistinct, discontinuous reflectors. It is interesting that the number of ash layers/m.y. roughly correlates with these subunits (see Fig. 10).

As we found at Sites 578 and 579, the compressional wave velocity profile for Site 580 is dominated by high

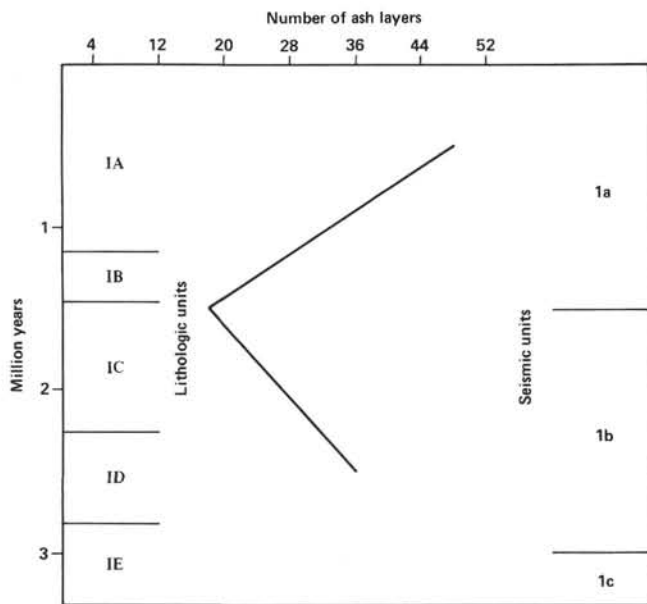


Figure 10. Plot of number of ash layers accumulated per million years at Site 580.

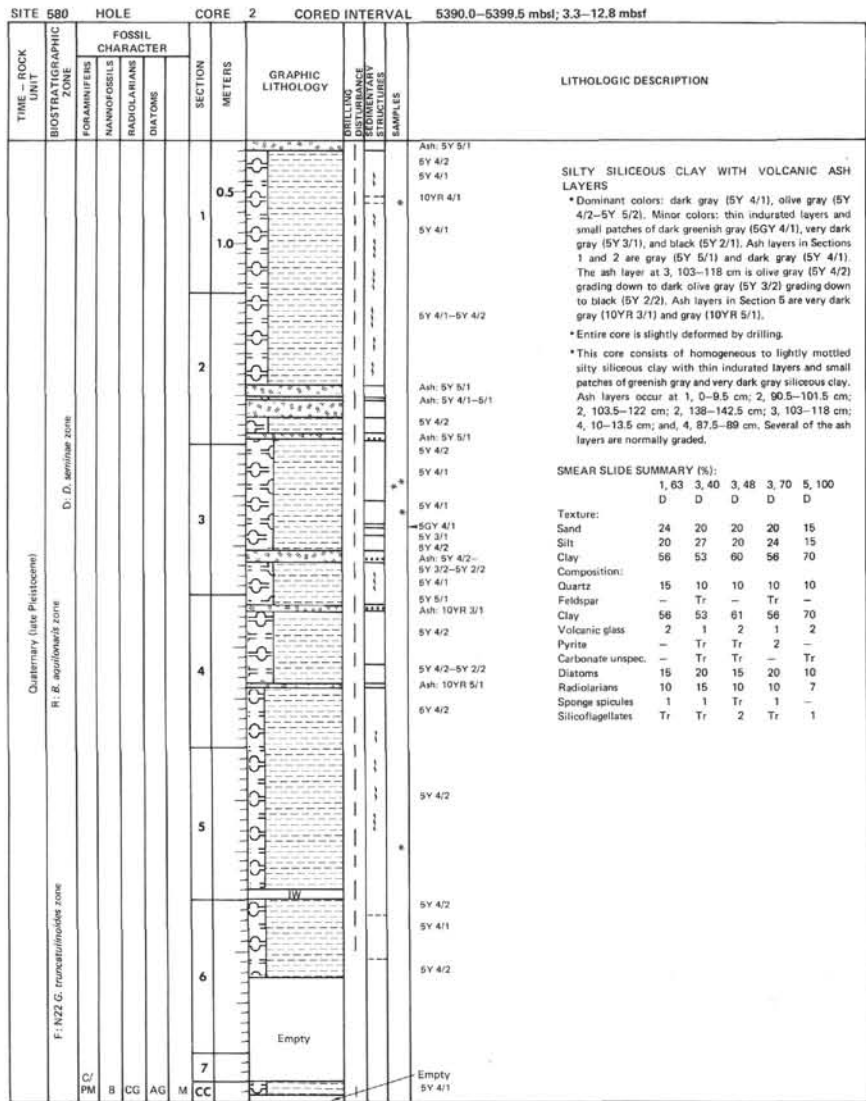
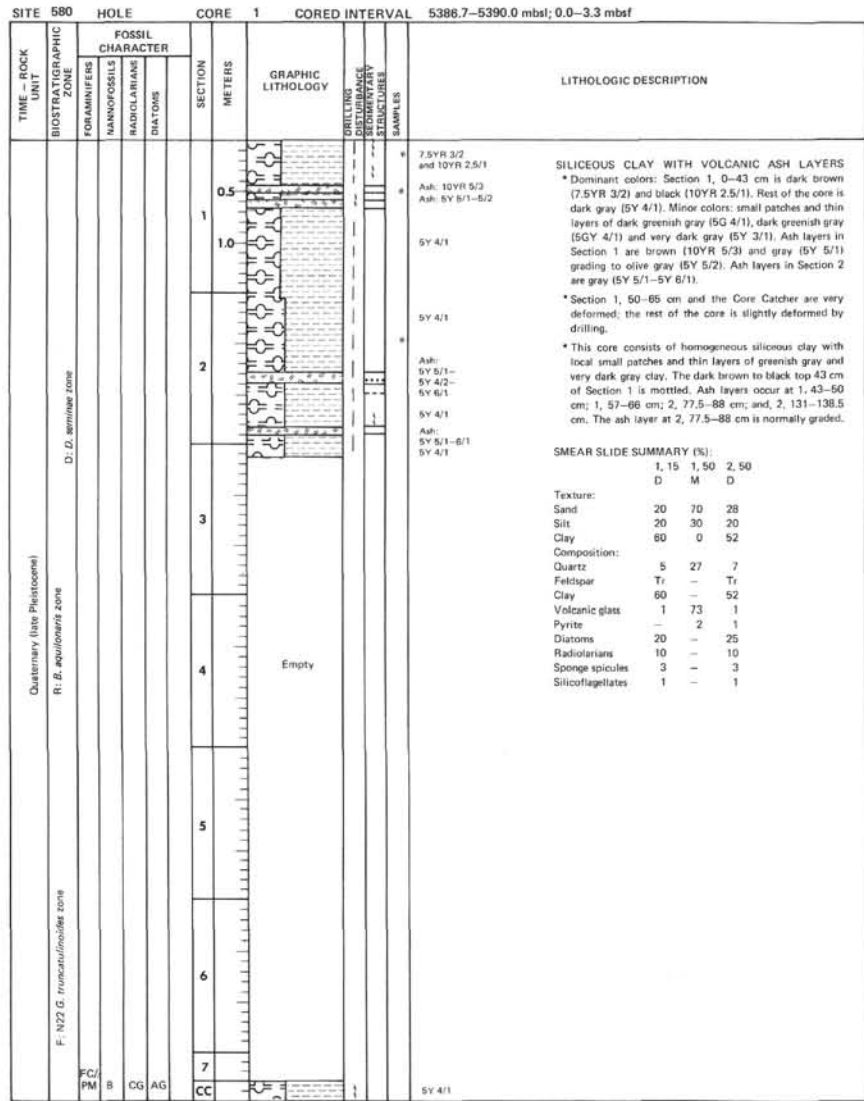
velocity, semi-indurated greenish clay and ash layers. Velocities rise gradually downhole from 1.47 to 1.49 km/s in the siliceous clays and oozes. Detailed velocity profiles obtained on five ash layers clearly show that, for some layers, the maximum velocity occurs at or near the sharp, basal contact.

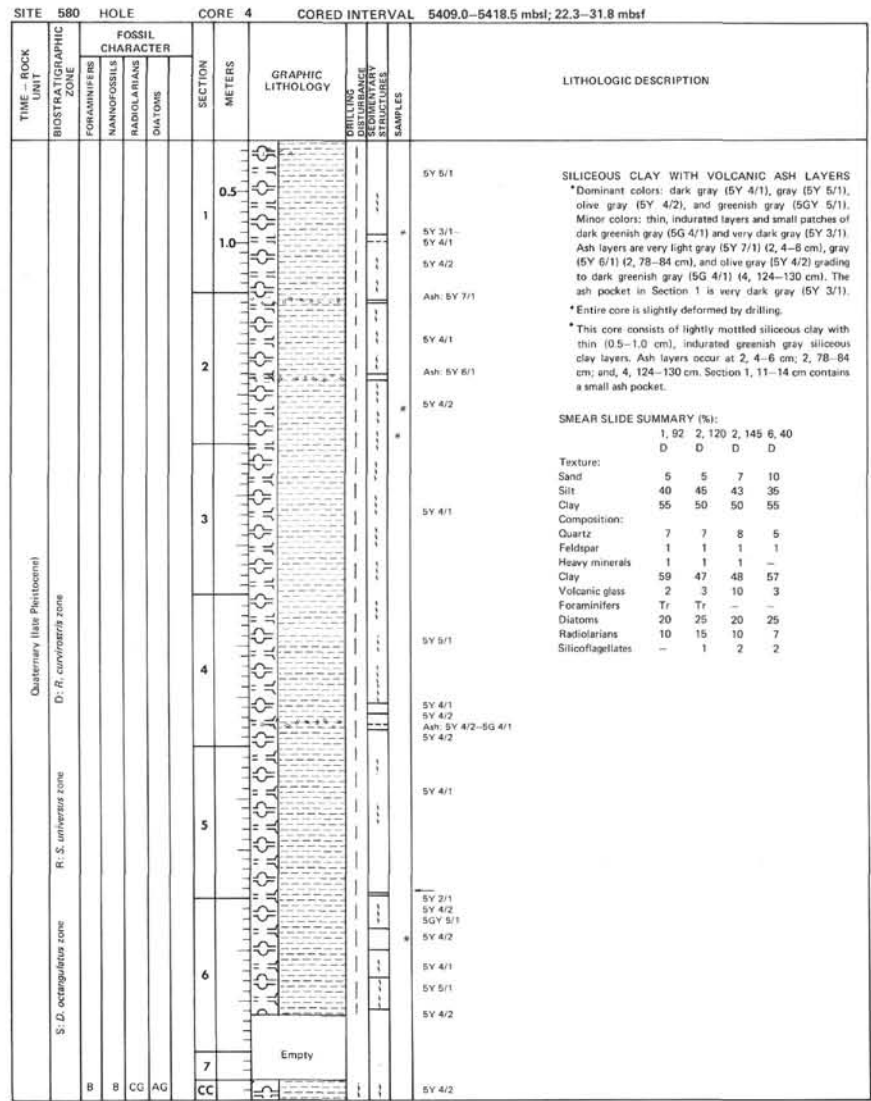
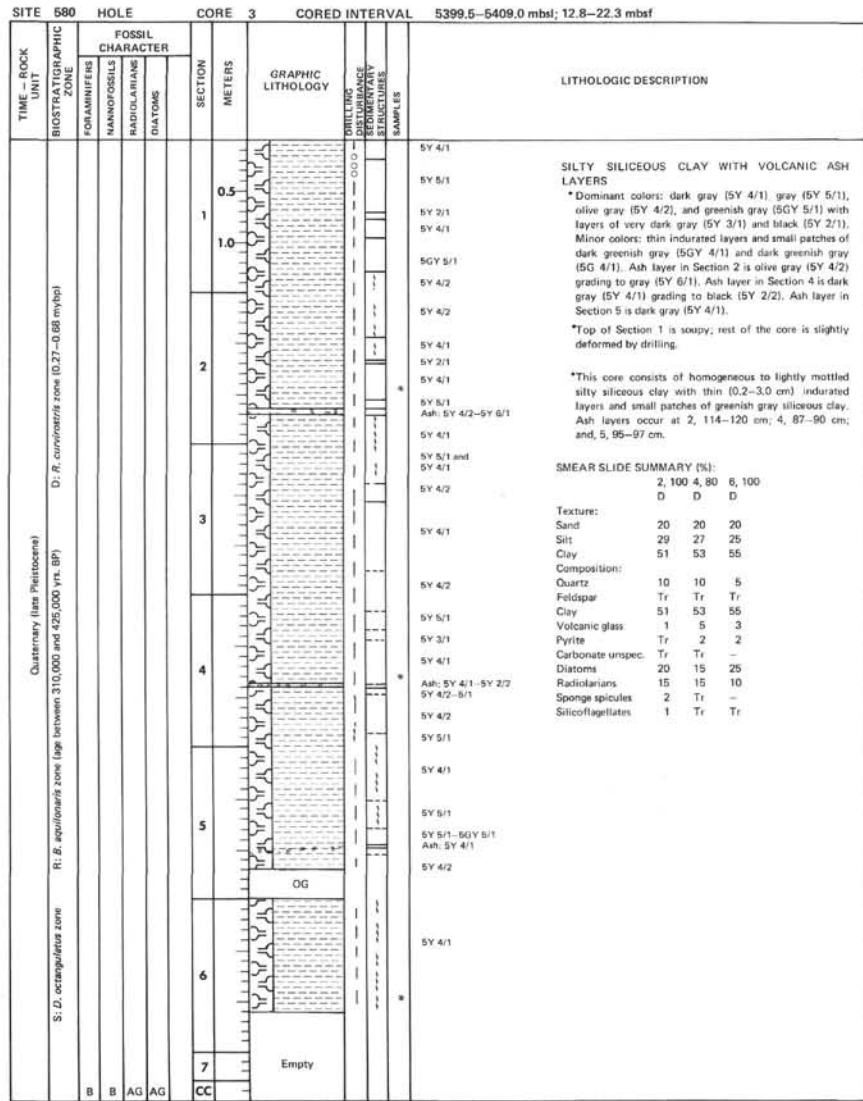
A total of eleven heat flow measurements were taken at Site 580. Measurements began at 22.3 m sub-bottom depth and continued to a sub-bottom depth of 155.3 m. Except for one anomalous point at 70 m, the data show a fairly linear increase in temperature with depth.

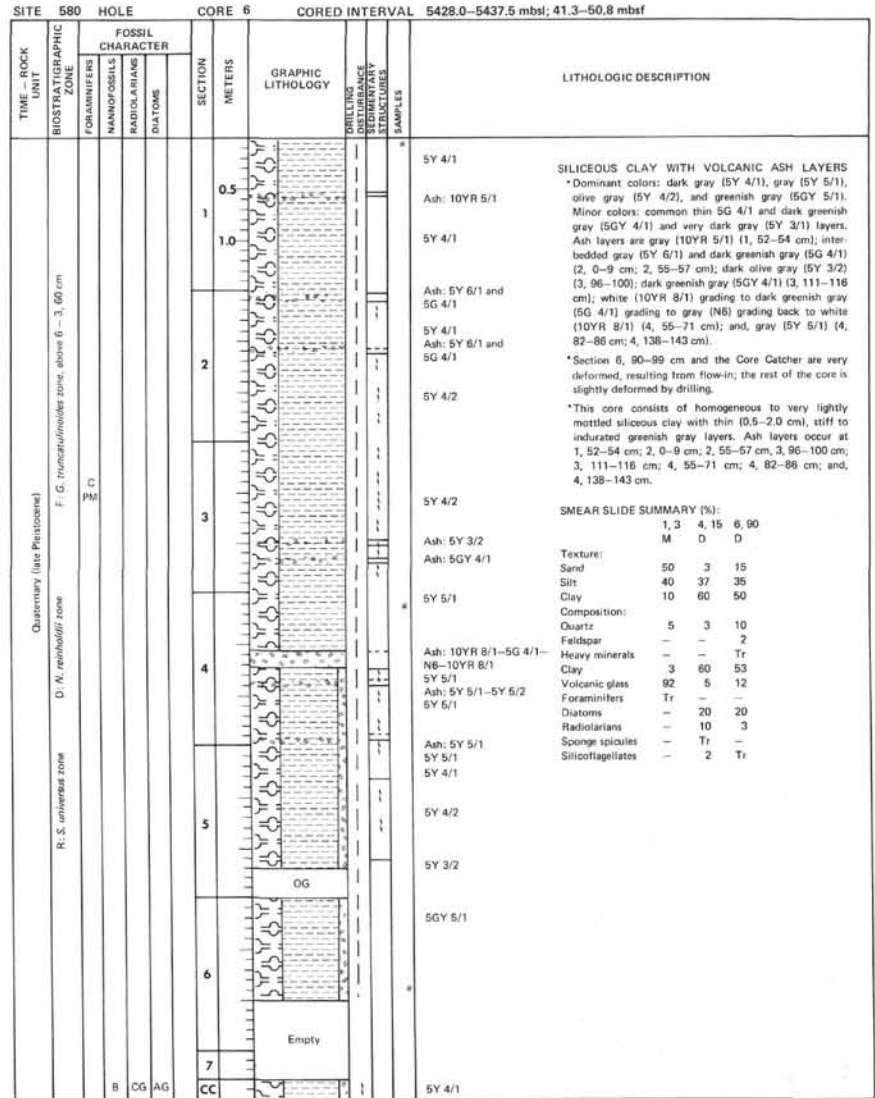
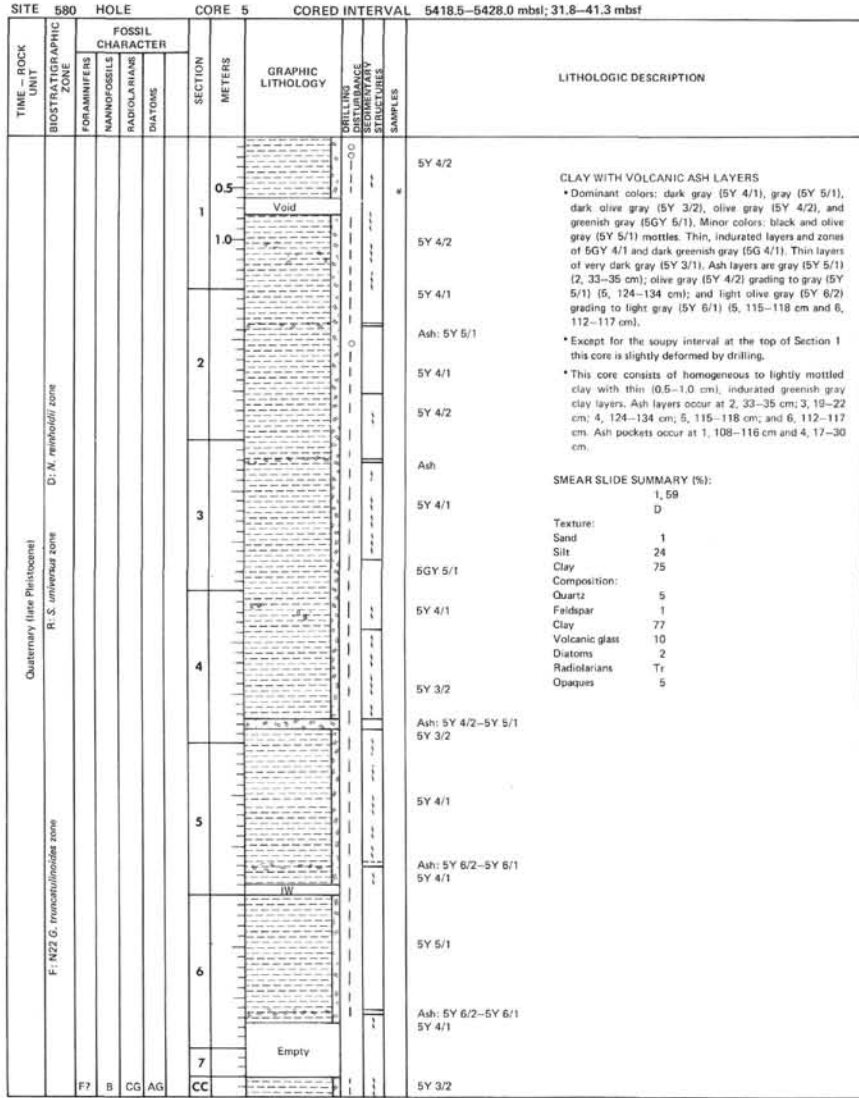
The objectives for this site—to obtain a detailed paleoceanographic record in the subtropical-subarctic gyre transition zone for the late Cenozoic; to refine the mid-latitude stratigraphy using paleomagnetism, tephrochronology, and biostratigraphy; to determine the time of onset of significant biosiliceous accumulation; to determine the timing and nature of the onset of the mid-Pliocene and Pleistocene climatic deterioration; to assess the nature and history of authigenic sedimentation in pre-biosiliceous sediments; and to determine the Cenozoic history of eolian sedimentation for comparison with sites to the south and north—was only partly achieved. Because of time limitations, we were unable to core as deep as our objectives required.

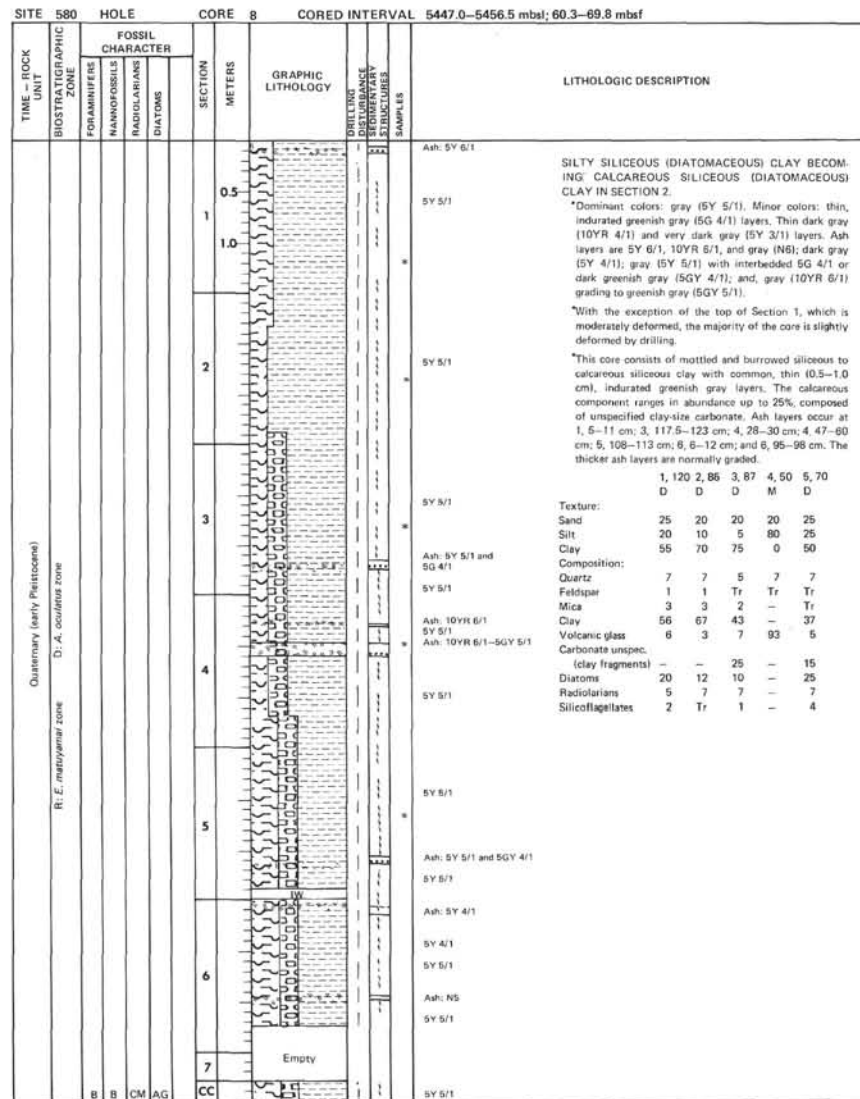
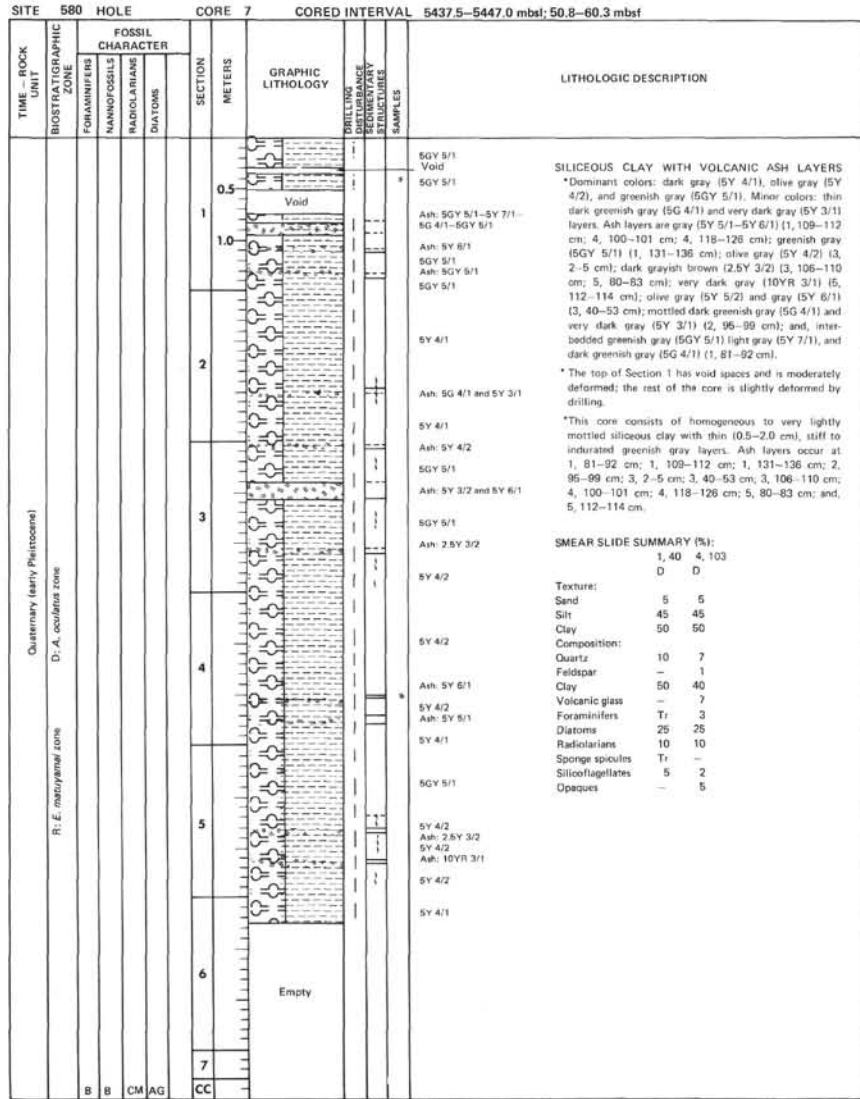
REFERENCES

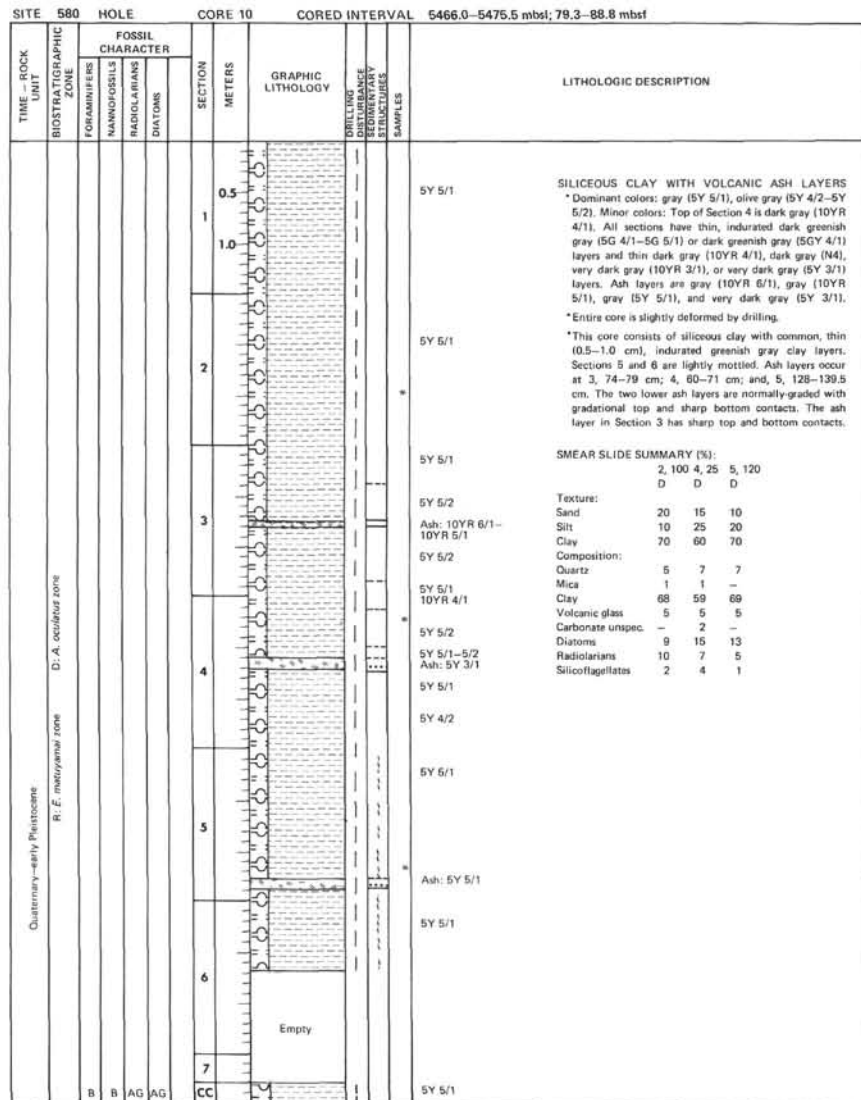
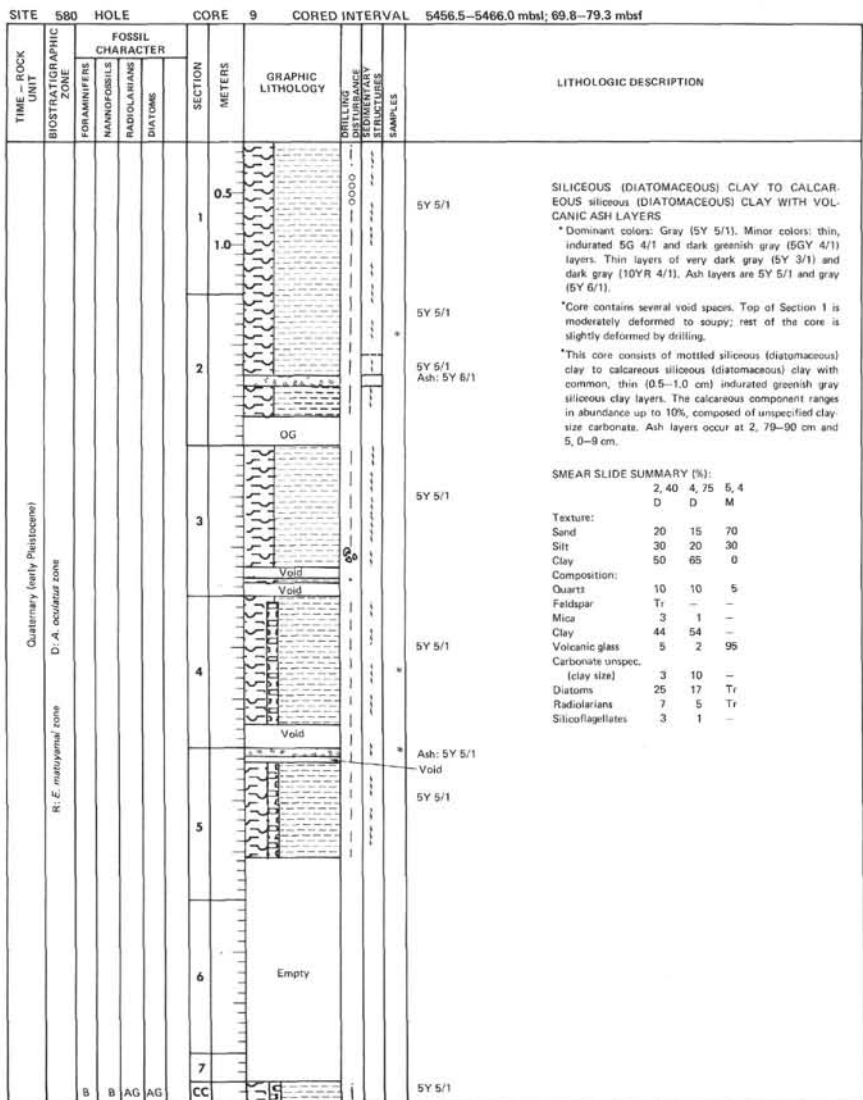
- Berggren, W. A., Kent, D. V., and Flynn, J. J., in press. Paleogene geochronology and chronostratigraphy. In Snelling, N. J. (Eds.), *Geochronology and the Geological Record*. Geol. Soc. London Spec. Pap.
- Blow, W. H., 1969. Late middle Eocene to Recent planktonic foraminiferal biostratigraphy. In Brönnimann, P., and Renz, H. H. (Eds.) *Proc. First Int'l. Conf. Planktonic Microfossils* (Vol. 6): Leiden (Brill), 199–422.
- Boyce, R. E., 1976a. Definitions and laboratory techniques of compressional and sound velocity parameters and wet-water content, wet-bulk density, and porosity parameters by gravimetric and gamma ray attenuation techniques. In Schlanger, S. O., Jackson, E. D., et al., *Init. Repts. DSDP, 33*: Washington (U.S. Govt. Printing Office), 931–958.
- , 1976b. Deep Sea Drilling Project procedures for shear strength measurements of clayey sediment using modified Wykeham Farrance Laboratory Vane Apparatus. In Barker, P. F., Dalziel, I. W. D., et al., *Init. Repts. DSDP, 36*: Washington (U.S. Govt. Printing Office), 1059–1068.
- Foreman, H. P., 1973. Radiolaria from DSDP Leg 20. In Heezen, B. C., MacGregor, I. D., et al., *Init. Repts. DSDP, 20*: Washington (U.S. Govt. Printing Office), 249–305.
- , 1975. Radiolaria from the North Pacific, Deep Sea Drilling Project, Leg 32. In Larson, R. L., Moberly, R., et al., *Init. Repts. DSDP, 32*: Washington (U.S. Govt. Printing Office), 579–701.
- Furuta, T., and Arai, F., 1980. Petrographic properties of tephros, Leg 56, Deep Sea Drilling Project. In Scientific Party, *Init. Repts. DSDP, 56, 57, Pt. 2*: Washington (U.S. Govt. Printing Office), 1043–1048.
- Hays, J. D., 1970. Stratigraphy and evolutionary trends of Radiolaria in North Pacific deep-sea sediments. In Hays, J. D. (Ed.), *Geological Investigations of the North Pacific*. Mem. Geol. Soc. Am., 126:185–218.
- Koizumi, I., 1973. The late Cenozoic diatoms of Sites 183–193, Leg 19, Deep Sea Drilling Project. In Creager, J. S., Scholl, D. W., et al., *Init. Repts. DSDP, 19*: Washington (U.S. Govt. Printing Office), 805–855.
- Stainforth, R. M., Lamb, J. L., Luterbacher, H., Beard, J. H., and Jeffords, R. M., 1975. Cenozoic planktonic foraminiferal zonation and characteristics of index forms. *Univ. Kans. Paleontol. Contrib. Pap.*, 62:1–425.

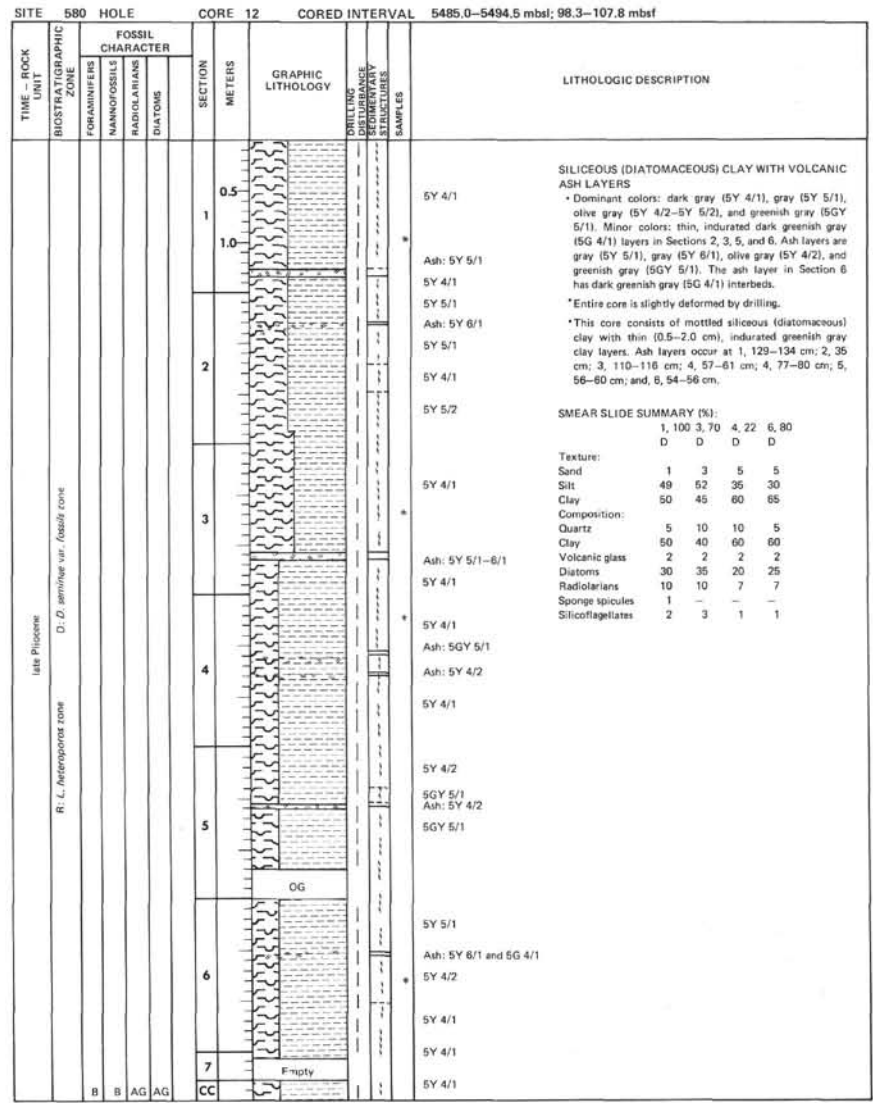
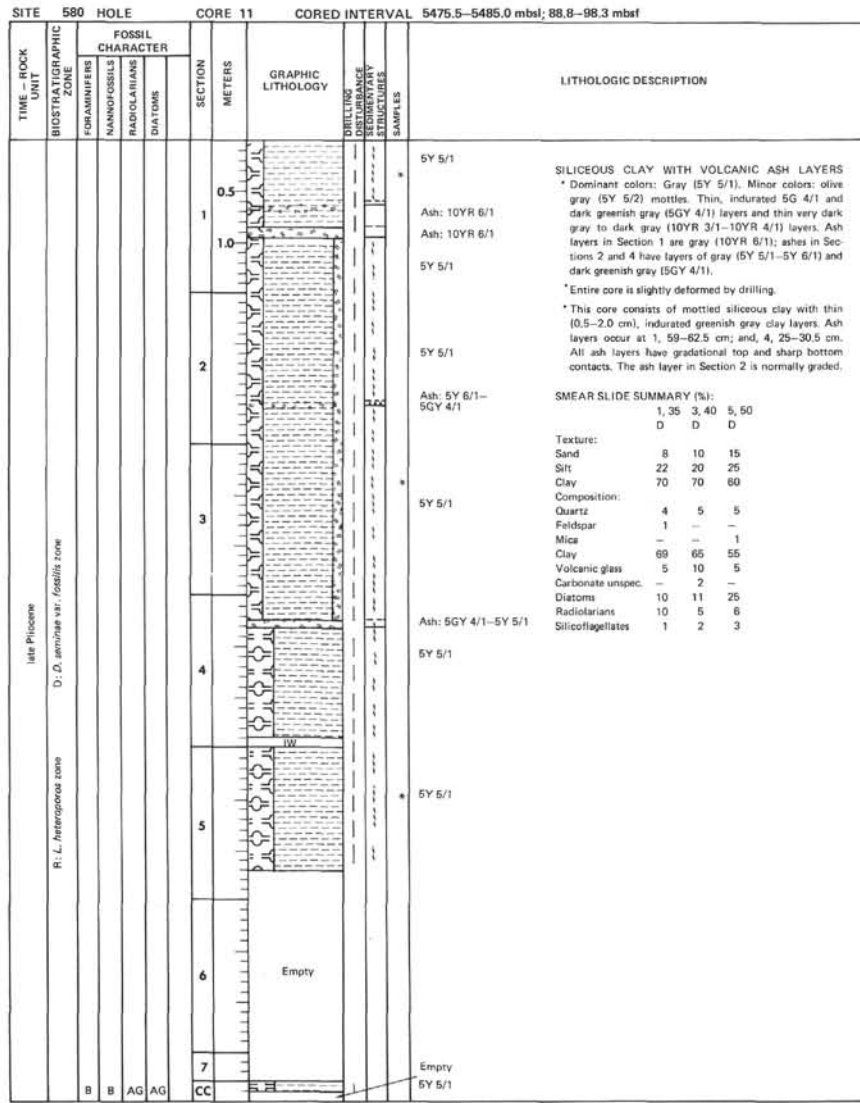


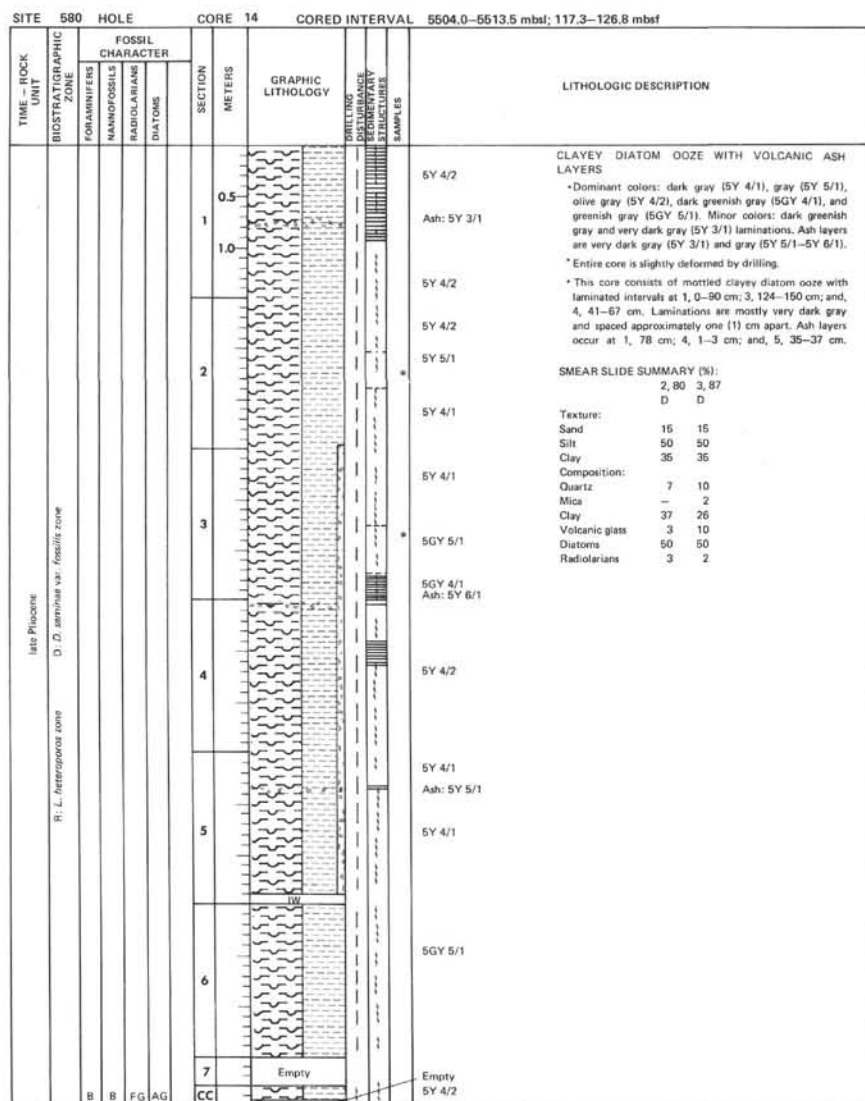
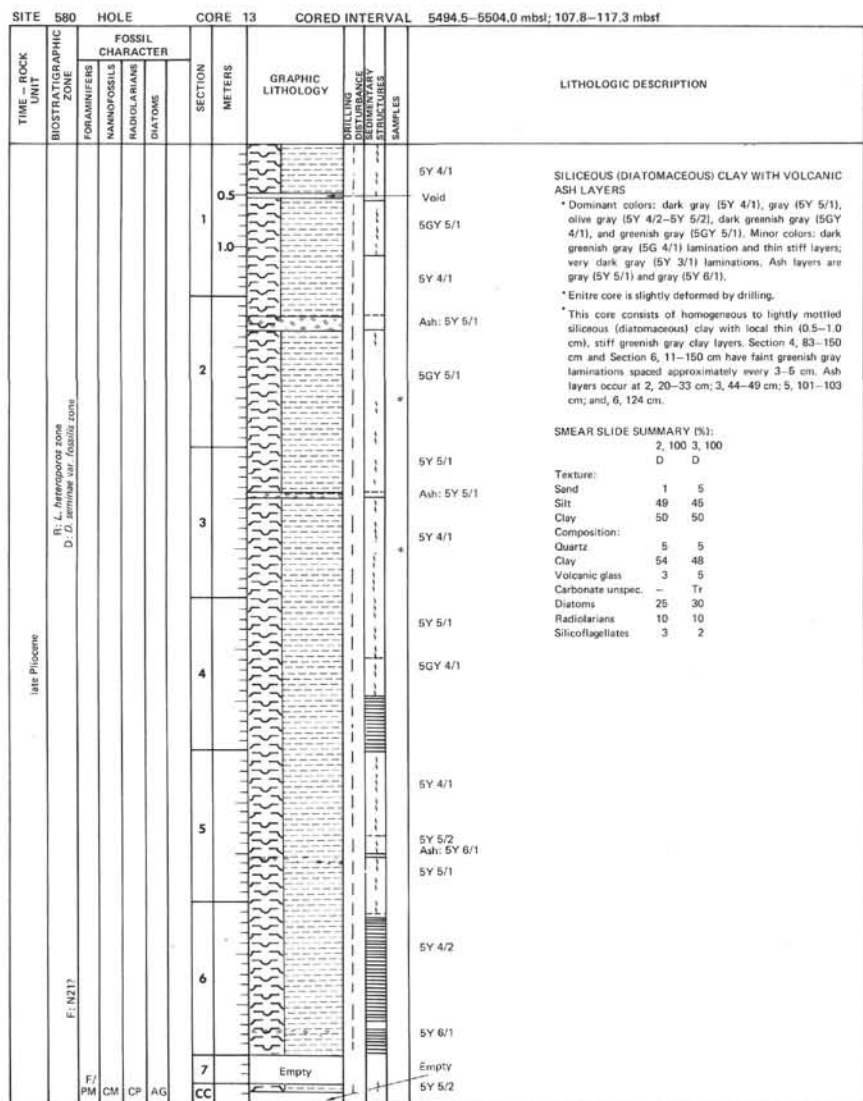


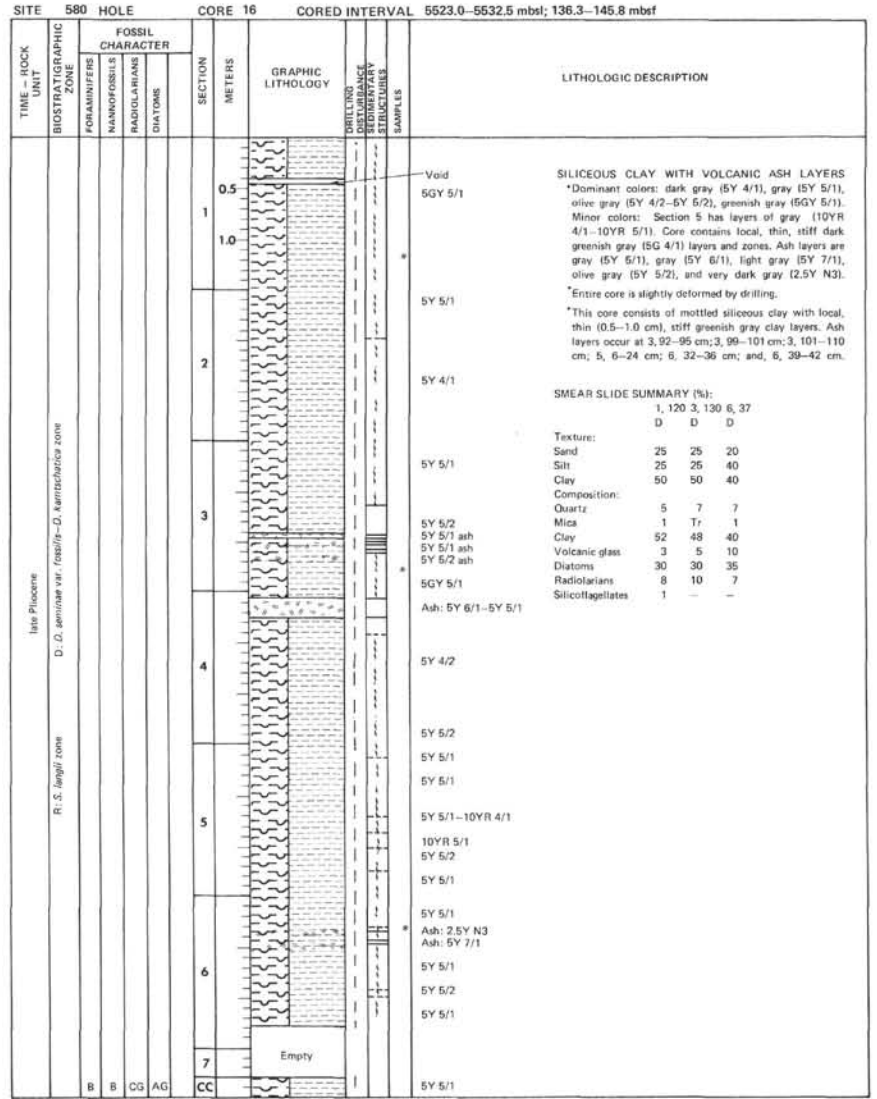
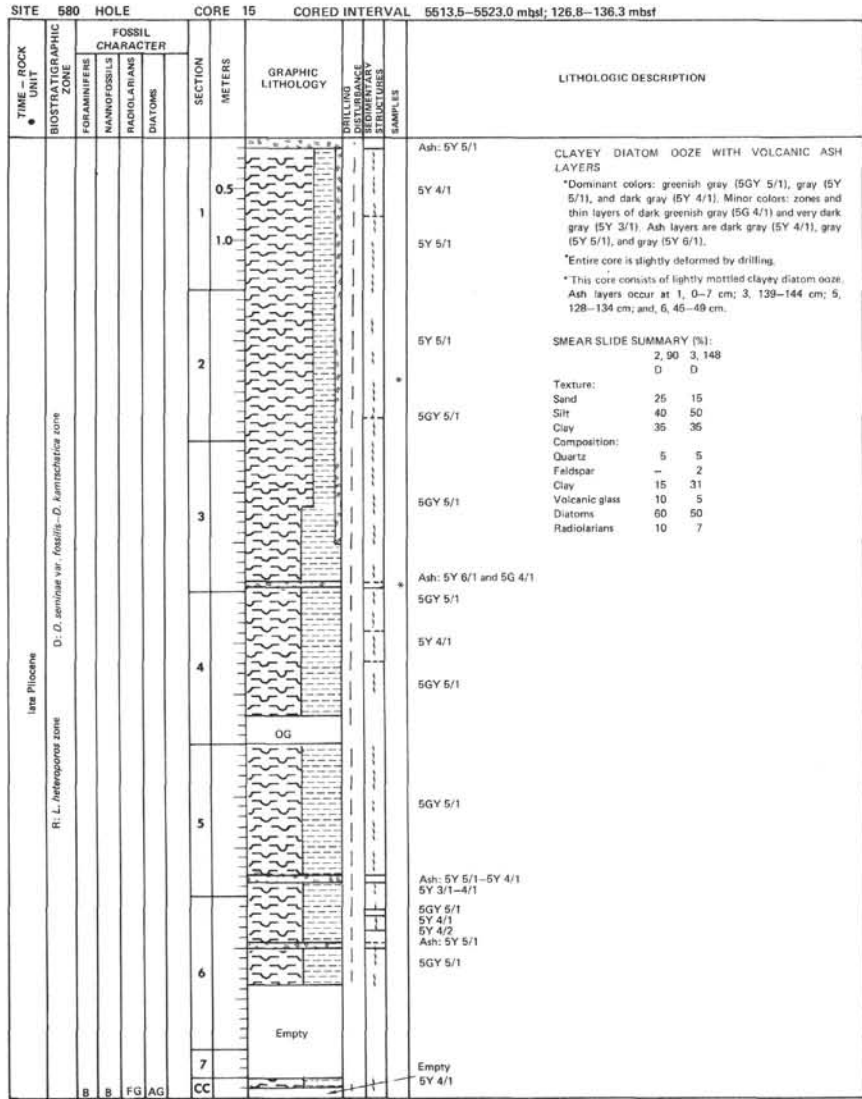












SITE 580 HOLE CORE 17 CORED INTERVAL 5532.5-5642.0 mbsf; 145.8-155.3 mbsf

